Ip25: A Molecular Proxy of Sea-ice Duration in the Bering and Chukchi Seas

IP_{25}: A MOLECULAR PROXY OF SEA-ICE DURATION

IN THE BERING AND CHUKCHI SEAS

A thesis presented

by

CECILY JANE SHARKO

**Submitted to the Graduate School of the
University of Massachusetts Amherst in partial fulfillment
of the requirements for the degree of**

MASTER OF SCIENCE

September 2010

Department of Geosciences

IP$_{25}$: A MOLECULAR PROXY OF SEA-ICE DURATION

IN THE BERING AND CHUKCHI SEAS

A thesis presented

By

CECILY JANE SHARKO

Approved as to style and content by:

____
Julie Brigham-Grette, Chair

____
Steven Petsch, Member

____
Robert DeConto, Member

____
Mark Leckie, Member

____
Mark Leckie, Department Head
Department of Geosciences

ACKNOWLEDGMENTS

I would like to thank my advisor, Julie Brigham-Grette, for her support, guidance, and patience. I thank my committee member and laboratory supervisor, Steven Petsch, for his direction and instruction. I would also like to thank my committee members, Mark Leckie and Robert DeConto, for their helpful comments and suggestions throughout this study. I thank Beth Caissie for all her assistance, advice, and encouragement. I also greatly appreciate all the insights, ideas, and enthusiasm they shared, which aided in the success of this project.

Thank you to the Department of Geosciences at the University of Massachusetts Amherst for awarding me the Leo M. Hall Memorial Scholarship, which partially funded my project.

I would also like to extend my gratitude to all the former and current members of the University of Massachusetts Amherst Biogeochemistry Laboratory, Mark Woodworth, Jeffrey Salacup, Kenna Wilkie, Carrie Petrik-Huff, Tom Naughton, Addie Holland, Zhaohui Zhang, William D'Andrea, for all the knowledge, counsel, ideas, and laboratory duties we shared. I am also grateful to Guillaume Massé and the members of the LOCEAN laboratory at the Université Pierre et Marie Curie in Paris, France, for their hospitality and assistance with running samples.

A special thank you to my friends and family, especially my husband Tom, whose support and encouragement helped me to stay focused on my research and writing.

ABSTRACT

IP_{25}: A MOLECULAR PROXY OF SEA-ICE DURATION IN THE BERING AND CHUKCHI SEAS

SEPTEMBER 2010

CECILY JANE SHARKO, B.S., UNIVERSITY OF MISSOURI-ROLLA

M.S., UNIVERSITY OF MASSACHUSETTS AMHERST

Directed by: Professor Julie Brigham-Grette

Seasonal sea ice is an important component of the global climate system. Sea ice influences exchange rates of heat, moisture, and gas between the ocean and atmosphere. Sea ice also plays critical roles in high latitude ecosystems and marine carbon cycling. Records of sea-ice extent and duration in the Arctic Ocean and its marginal seas through geologic time are valuable resources for better understanding the intricate relationships between sea ice and climate.

IP_{25}, a compound biosynthesized exclusively by diatoms associated with sea ice, has been used to construct qualitative records of sea ice from sediment cores in some areas of the Arctic. However, IP_{25} has not previously been applied to sediments from the Bering and Chukchi Seas. This area exhibits a wide range of interannual seasonal ice duration, which makes the region a promising natural laboratory for developing a quantitative core-top calibration between sea ice and the IP_{25} biomarker.

A sample suite of surface sediments from the Bering and Chukchi Seas representing a range of latitudes (60-72^{o} N) and durations of sea ice per year (0.5-11 months/year) are analyzed for this study. Gas chromatography/mass spectrometry analysis of sediment solvent extracts reveals the presence of IP_{25} in all samples and

higher IP_{25} concentrations in the Chukchi Sea compared to in the Bering Sea. IP_{25} concentrations are compared with data for several sea surface conditions: mean annual sea-ice duration, sea surface temperature and salinity, and insolation data. An exponential relationship between TOC-normalized IP_{25} concentration and average annual duration of sea ice is identified. Negative exponential relationships are identified between IP_{25} and the other sea surface conditions: average annual and August sea surface temperature and average annual and August sea surface salinity. Exponential relationships are also identified between TOC-normalized IP_{25} concentrations and insolation, and insolation coupled with sea-ice concentration.

IP_{25} in surface sediments is a viable quantitative proxy for sea-ice duration in the Bering and Chukchi Seas. However, sea surface conditions, such as temperature, salinity, sea-ice duration/concentration, and insolation are not independent variables. Therefore it is difficult to determine which of these environmental factors has/have the most influence on IP_{25} production. Further research and statistical analysis may serve to refine these relationships.

TABLE OF CONTENTS

Page

LIST OF FIGURES

CHAPTER 1

LITERATURE REVIEW

1.1. Introduction

Polar sea ice has an intimate and complex relationship with global climate. This reflects the interplay between ice thickness, extent, and duration and the exchange of heat, moisture, and gas between the ocean and atmosphere. Therefore, changes in these ice characteristics both drive and reflect climatic changes. One role sea ice plays in heat exchange is keeping the atmosphere cool by reflecting solar radiation (Royer et al., 1990, Parkinson et al., 2001). Sea ice has a high surface albedo, which limits short-wave radiation absorption that would otherwise heat the ice and ocean surface. Sea ice also emits long-wave radiation, which cools the ice and ocean surface and the air blowing across them (Dieckmann and Hellmer, 2003). More intense sea-ice conditions keep the atmosphere cooler, and a cooler atmosphere allows for more intense sea-ice conditions. Sea-ice formation can also cool and, through brine rejection, increase the salinity of surface waters in polar oceans (Dieckmann and Hellmer, 2003). In the North Atlantic, these colder, denser water masses sink to become bottom waters that contribute to thermohaline circulation (Broecker, 1997; McBean et al., 2005). In this way, sea-ice formation and degradation play pivotal roles in determining rates of global ocean circulation, which is responsible for transferring cold water equatorward and warm water poleward. Sea-ice presence at particular locations can also strengthen/weaken atmospheric circulation and pressure, and thus affect storm intensity and precipitation (Budikova, 2009). Sea ice also plays a critical role in high latitude carbon cycling, which also affects global climate. Sea-ice algae can uptake carbon faster than pelagic phytoplankton (Lee et al., 2008) and melting sea ice sheds its organic matter suddenly allowing for faster carbon burial rates (Riedel et al., 2006).

Reconstruction of Arctic sea-ice conditions through geologic time is a valuable tool for examining the relationship between sea ice and changes in climate. It can also demonstrate how sea-ice fluctuations have driven and reflected climatic change in the past. A better understanding of how changes in sea-ice conditions, particularly extent and duration, have affected past climates allows us to understand how the presence or absence of sea ice will affect our present and future climate.

1.2. Background Information

1.2.1. Location geography and sea-ice

This project focuses on the development of a quantitative molecular proxy for sea-ice extent/duration in Bering and Chukchi Sea surface sediments. The Bering Sea is a marginal sea located in the subarctic Pacific Ocean and the Chukchi Sea lies just over the Arctic Circle to the north. Both are bounded by northeast Russia to the west and Alaska to the east. The Aleutian Islands and the Bering Strait comprise the Bering Sea's southern and northern boundaries, respectively, and the Chukchi Sea lies just north of the Bering Strait (Figure 1.1). The Bering and Chukchi Seas' location in a subpolar/polar region makes them important sites of seasonal sea-ice formation.

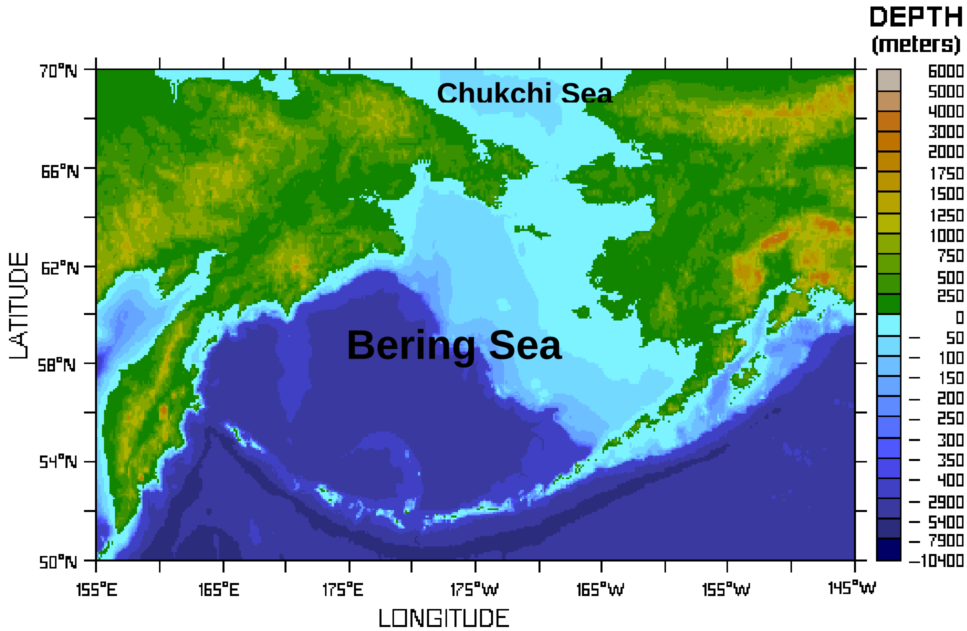

Figure 1.1. Bathymetry of the Bering Sea
(Image courtesy of NOAA Pacific Marine Environmental Laboratory)
http://disc.gsfc.nasa.gov/oceancolor/scifocus/oceanColor/bering_sea.shtml

Sea ice in the Bering and Chukchi Seas contributes to the total extent of sea ice in the Northern Hemisphere. In modern times, Bering Sea ice has extended southward approximately to the shelf break, and sea-ice duration has ranged from approximately 0.5 month/year at the southernmost ice edge to 9 months/year near the Bering Strait. Chukchi Sea ice has extended southward to the Bering Strait and has lasted 8-11 months/year, increasing from south to north (Edwards, 1989; NASA, 1992; NSIDC, 1992; 1993).

1.2.2. Sea-ice microalgae

Sea ice offers a unique environment in which many polar microbial organisms thrive and flourish (Horner, 1985). Depending on the type of organism, the amount of nutrients and sunlight it requires to live, and ice density, thickness, and duration, sea-ice microorganisms can live in a variety of places in the ice: pools of sea water on the surface, brine pockets within, and attached to the underside (Arrigo, 2003). Sea-ice microbiota include diatoms, dinoflagellates, foraminifera, bacteria, and archaea (Gradinger et al., 1999). Sea-ice algae, specifically diatoms, dominate sea-ice blooms (Riedel et al., 2008). Sea ice provides a floating platform to which sea-ice algae can attach themselves and remain in the surface waters of the ocean, where there are greater amounts of nutrients and greater access to sunlight essential for survival and growth, than there are further down the water column (Arrigo, 2003).

Arctic sea-ice diatoms bloom in the spring starting at the ice edge and propagate northwards as the sea ice recedes through the spring and summer (Alexander and Niebauer, 1981). The bloom is when the most primary productivity takes place, and as the ice melts, organic material from the sea ice is shed into the underlying water column and is eventually deposited into the sediment record. In this study site, the ice algal bloom starts at the southern Bering Sea ice-edge in April and progresses northward into the Chukchi Sea as the ice-edge retreats through May/June (Wang et al., 2005; Rho and Whitledge, 2007; Lalande et al., 2007). Diatoms are incorporated into the sea ice starting in late fall as the surface water begins to freeze and solidify (Gradinger and Ikävalko, 1998). The diatoms photosynthesize very minimally during these cold, dark months (Horner, 1985). However, in the early spring, once daily hours of sunlight increase, photosynthesis and the net production of organic compounds increase (Horner and Schrader, 1982; Rochet et al., 1986). Increasing availability of sunlight is one of the most important factors that initiates and drives the spring bloom (Horner and Schrader, 1982; Niebauer et al., 1990). As the bloom propagates northward later in the spring and through the summer, the hours of daily sunlight increase as well. Therefore, the Chukchi Sea ice algae have more sunlight available when they bloom later in the season than ice algae in the Bering Sea at the time of their earlier bloom.

Sea-ice diatoms alter their biochemistry in response to these annual environmental changes (Lizotte, 2003). They adapt to their changing environment, particularly changing solar insolation, by preferentially biosynthesizing certain organic compounds. At times of decreasing/lower irradiances, such as during the late fall and winter, some sea-ice algae preferentially synthesize more protein than polysaccharides (McConville, 1985), which may be a method to reinforce cellular membranes. This membrane reinforcement may be merely a response to decreased light availability or an adaptation to colder temperatures (McConville, 1985) as insolation and temperatures both decrease. Some sea-ice diatoms have been known to increase carbon allocation to glycolipids, a component of thylakoid membranes of chloroplasts, to enhance photosynthetic efficiency in low-irradiance conditions (Arrigo, 2003). However, as solar irradiance increases through the spring and summer months, sea-ice diatoms decrease carbon allocation to proteins in favor of lipids and soluble polysaccharides (Smith et al., 1987; 1989). Furthermore, sea-ice algae preferentially allocate carbon to structural lipids (e.g. membrane phospholipids) in early spring and as solar irradiance increases, allocate more of their carbon to storage lipids (e.g. triglycerides) (McConville, 1985; Arrigo, 2003).

1.2.3. Contributions of sea-ice microalgae to high latitude ecosystems and carbon cycling

Sea-ice algae are important to polar ecosystems because they are often the only source of fixed carbon for higher organisms in over-winter ice-covered seas (Thomas and

Dieckmann, 2003). Even when pelagic phytoplankton are present, sea-ice algae have been known to contribute more than half of the total primary productivity (Horner and Schrader, 1982; Gosselin et al., 1997; Lee et al., 2008) Their dominance in blooms of ice-covered seas makes sea-ice algae an important food and carbon source for higher trophic levels, particularly in winter months when there is negligible pelagic phytoplankton (Michel et al., 1996; Leventer, 2003). Pelagic zooplankton graze on ice algae directly, but algal matter shed from the ice as it melts can also sink through the water column and provide food to benthic organisms as well (Lee et al., 2008). Sea-ice algae cannot live and produce this much needed food/carbon source without the presence of sea ice, making sea ice itself invaluable to the maintenance of the Bering and Chukchi Seas high productivity and the survival of its ecosystems (Gosselin et al., 1997; Stabeno et al., 2001).

Sea-ice algae's productivity and carbon contribution are also important to high latitude carbon cycling. In ice-covered seas, ice algae uptake carbon faster than pelagic phytoplankton (Lee et al., 2008). Organic matter from sea-ice algae also tends to form aggregates as it is shed from melting ice, allowing the organic matter to be deposited to the sediment faster (Leventer, 2003). Some species of ice algae produce a 'sticky' extracellular polysaccharide mucilage that allows them to attach to their ice substrate (Riebesell et al., 1991; Leventer, 2003). Organic matter from other sources, such as bacteria, will accumulate on these sticky ice algal cells leading to faster sinking velocities for those larger particles (Riedel et al., 2006). The downward flux of sea-ice organic matter is also increased through zooplankton grazing and fecal pellet transport (Leventer, 2003).

1.2.4. Biogeochemistry of marine microorganisms

The marine microorganisms that support high production rates and diverse ecosystems also provide useful tools for geochemical paleoenvironment and paleoclimate reconstructions. When marine microorganisms die, their remains fall to the ocean floor and the constituent compounds that are most resilient to degradation, lipids, are preserved in the sediment record. The presence and abundance of various types of lipid compounds reveal different characteristics of the environment in which the lipids were deposited.

Alkenones are one of these types of lipid compounds. Alkenones are methyl and ethyl ketones with 37, 38, or 39 carbon atoms (C_{37}-C_{39}) and have 2, 3, or 4 double bonds (di-, tri-, and tetra-unsaturated) (Brassel et al., 1986; Prahl and Wakeham, 1987; Rosell-Mele, 1998) (Figure 1.2). Alkenones are biosynthesized by some coccolithophorid phytoplankton of the class Prymnesiophyceae (Brassel et al., 1986; Prahl and Wakeham, 1987). Most common among these alkenone-producing algae are *Emiliana huxleyi* and *Gephyrocapsa* spp. These phytoplankton live in the photic zone and produce alkenones with varying degrees of unsaturation (number of double bonds) in response to changes in sea surface temperature (SST). The degree of unsaturation is preserved in the alkenones at the time of phytoplankton death and thus preserves a record of SST at that time. The alkenone unsaturation index, U^{K}_{37}, first described by Brassel et al. (1986) is defined as the relative abundance of $C_{37:2}$, $C_{37:3}$, and $C_{37:4}$ alkenones in a sediment sample, expressed by:

$$U^{K}_{37} = [C_{37:2} - C_{37:4}] / [C_{37:2} + C_{37:3} + C_{37:4}]$$

The $C_{37:4}$ alkenone often occurs in negligibly small amounts and often cannot be detected, so Prahl and Wakeham (1987) simplified the equation to:

$$U^{K'}_{37} = [C_{37:2}] / [C_{37:2} + C_{37:3}]$$

The coccolithophorids produce more $C_{37:3}$ alkenones relative to $C_{37:2}$ alkenones at lower temperatures. Therefore, higher growth temperatures yield higher $U^{K'}_{37}$ values and conversely, lower growth temperatures yield lower $U^{K'}_{37}$ values (Brassel et al., 1986; Prahl and Wakeham, 1987; Prahl et al., 1988).

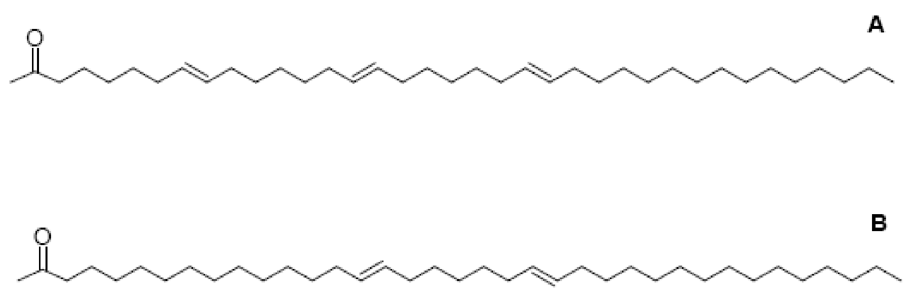

Figure 1.2. Chemical structures of $C_{37:3}$ (A) and $C_{37:2}$ (B) alkenones used in the alkenone unsaturation index ($U^{K'}_{37}$).

Numerous calibration studies have been performed to numerically relate this $U^{K'}_{37}$ value to sea surface temperatures so that it can be used to reconstruct SSTs of the past. Prahl and Wakeham (1987) grew cultures of *E. huxleyi* in various water temperatures and calculated $U^{K'}_{37}$ values grown at each temperature. They found a positive linear correlation between growth temperature and $U^{K'}_{37}$. Prahl et al. (1988) refined this correlation by considering a greater number of *E. huxleyi* cultures. The correlation equation they calculated is:

$$U^{K'}_{37}=0.034T + 0.039, (r^2=0.994),$$

where T=growth temperature in ^{o}C. Sikes et al. (1997) used core-top sediment samples from the subpolar Southern Ocean and calculated:

$$U^{K'}_{37}=0.038T - 0.082, (r^2=0.960)$$

for a $U^{K'}_{37}$ calibration for much colder waters. Muller et al. (1998) proposed a global core-top calibration involving sediment samples from 370 sites throughout the Atlantic, Pacific, and Indian Oceans. The equation for this set of data is:

$$U^{K'}_{37}=0.033T + 0.044, (r^2=0.958)$$

More recently, Conte et al. (2006) examined alkenone data from 630 surface water particulate samples and from over 700 surface sediment samples worldwide. These data, together with measured and annually averaged sea surface temperatures, were used to calculate global sea surface temperature calibration equations. The calibration derived from the coretop sediment data relates annual mean sea surface temperature (AnnO) to $U^{K'}_{37}$ with the equation:

$$AnnO=29.876(U^{K'}_{37}) - 1.334, (r^2=0.97)$$

The relationship between $U^{K'}_{37}$ values and sea surface temperature varies according to the alkenone data source, i.e. surface water particulates, laboratory cultures, surface sediment. Alkenones collected from laboratory cultures of algae yield more direct and more controlled growth temperature data than those collected from water or sediment samples. Therefore, discrepancies between $U^{K'}_{37}$ values and growth temperature can be investigated. Prahl et al. (2003) and (2006) state that non-thermal conditions, such as nutrient deficiency and light deprivation, affect the relative abundances of alkenones produced by algae and therefore also affect the temperature signal from $U^{K'}_{37}$. Despite this, alkenones collected from surface water and sediment can still be accurately used to estimate mean annual SSTs using $U^{K'}_{37}$ because it provides a mean temperature for the year, and not a specific growth temperature (Prahl et al., 2006).

Harada et al. (2003) examined the concentrations of C_{37} alkenones in the eastern Bering Sea and applied the $U^{K'}_{37}$ index in this region. Alkenones were found in particulate matter and surface sediments and their relative abundances used to find $U^{K'}_{37}$ values. SSTs were calculated using the calibration equations of Prahl et al. (1998), Sikes et al. (1997), and Muller et al. (1998) and compared to observed SSTs in the Bering Sea. Of these three calibrations, Sikes' et al. (1997) calibration provided the best correlation.

Membrane lipids produced by marine Crenarcheaota have also been discovered to provide a sea surface temperature proxy (Schouten et al., 2002). The specific lipids used in this proxy are called glycerol dialkyl glycerol tetraethers (GDGTs) and, like alkenones, their composition varies with growth temperature. However, unlike alkenones, whose unsaturation varies with growth temperature, the number of cyclopentane rings in GDGT molecules varies as a response to changes in growth temperature. Schouten et al. (2002) investigated the GDGT distribution in over 40 surface sediments worldwide. GDGTs with zero, one, two and three cyclopentane rings (GDGT 0-3 respectively) were identified in the sediment (Figure 1.3). Two other GDGT compounds were identified: crenarcheaol (GDGT 4) which has four cyclopentane rings and one cyclohexane ring, and a crenarcheaol regioisomer (GDGT 4') (Schouten et al., 2002; 2007; Sinninghe Damste et al., 2002) (Figure 1.3). Schouten et al. (2002) developed TEX_{86} (TetraEther index of GDGTs with 86 carbons) which is a measure of the relative abundances of GDGTs 1, 2 , 3, and 4', expressed as:

$$TEX_{86} = [2 + 3 + 4'] / [1 + 2 + 3 + 4']$$

Archaea biosynthesize GDGTs with increasing numbers of cyclopentane rings as growth temperature increases (Wuchter et al., 2004). Schouten et al. (2002) correlated TEX_{86} to annual mean SST using 40 surface sediments from 15 sites worldwide. The calibration equation calculated is:

$$TEX_{86} = 0.015T + 0.28, (r^2=0.92),$$

where T= annual mean SST in ^{o}C.

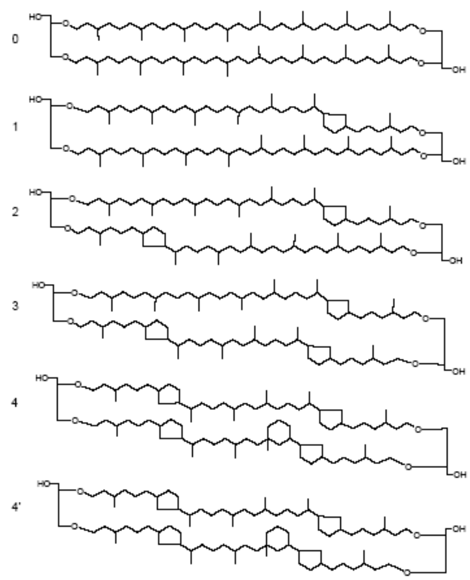

Figure 1.3. Chemical structures of glycerol dialkyl glycerol tetraethers (GDGTs) used in TEX_{86}. GDGTs 0,1,2, and 3 contain 0,1,2, and 3 cyclopentane rings respectively. GDGT 4 contains 4 cyclopentane rings and one cyclohexane ring. GDGT 4' is a region-isomer of GDGT 4.

Another class of biogeochemical compounds is highly branched isoprenoids (HBIs), which are C_{20}, C_{25} and C_{30} hydrocarbons built from C_5 isoprene units, and often exhibit one or more double bonds in their molecular structures. Highly branched isoprenoids are biosynthesized by some marine diatoms and have been detected in marine surface sediment and sediment cores from around the world (reviewed by Rowland and Robson, 1990; Hird et al., 1992). The diatom genera most often identified as the producers of HBIs include *Haslea* spp., *Rhizosolenia* spp., *Pleurosigma* spp. And

Navicula spp. (Volkman et al., 1994; Wraige et al., 1997; Belt et al., 2000; 2001; Xu et al., 2006).

The highly branched isoprenoids' diatom source allows them to be used to detect the presence of diatoms in marine environments and to distinguish organic matter input contributed by diatoms from organic matter from other sources (Belt et al., 2000; Xu et al., 2006). Gearing et al. (1976) uses differences in isoprenoid distributions to identify two distinct shelf environments in the Gulf of Mexico. HBIs characteristic of a terrestrial source are observed in surface sediments close to the shore, particularly the Mississippi River delta. Conversely, HBIs characteristic of a marine source are observed in surface sediments father from shore and the delta. In the same study, concentration ratios of two isoprenoids, pristane and phytane, in surface sediments are used to indicate areas of higher petroleum input to the sediments (Gearing et al, 1976). Hird et al. (1992) suggested that the positions of double bonds within C_{20} and C_{25} monoenes could be used to distinguish their source organism or environment in which the source organism lived, or both.

Further research has revealed various relationships between HBI characteristics, abundances, assemblages, number and position of double bonds, etc., and environmental conditions. Salinity has been found to affect the assemblages and concentrations of C_{25} alkenes in Shark Bay, Australia (Dunlop and Jefferies, 1985). In a study described in Wraige et al. (1998), it was observed that *Haslea ostrearia* cultures grown in 15 psu salinity produced a greater abundance of a C_{25} triene than those grown in 40 psu salinity. However, cultures grown between 25 and 35 psu salinities produced the highest concentrations of the triene of any cultures grown between 15 and 40 psu salinities. The effects of salinity on HBI production in cultures of *Rhizosolenia setigera* were investigated in Rowland et al. (2001b). In this study, cultures grown at 35 psu were observed to have experienced increased cell growth and increased C_{30} production, but decreased C_{25} production compared to cultures grown at 15 psu. It was further reported that the salinity increase did not affect the degree of unsaturation in C_{25} compounds, but the salinity increase did decrease the degree of unsaturation in the C_{30} compounds (Rowland et al., 2001b). Rowland et al., (2001a) grew cultures of *Haslea ostrearia* at different temperatures and reports that unsaturation (i.e. number of double bonds) increases in C_{25} compounds with increasing growth temperature. In a following study (Rowland et al., 2001b), similar results were reported for cultures of *Rhizosolenia setigera*. Similar to *Haslea ostrearia*, the *Rhizosolenia setigera* displayed an increase in C_{25} unsaturation with an increase in growth temperature from 18^{o}C to 25^{o}C. C_{30} unsaturation was also observed to increase with the same increase in growth temperature.

Important for the study proposed here, HBIs have also been found in sediments overlain by water containing sea ice for at least a portion of the year where diatoms make up an important component of marine primary production (Nichols et al., 1988; Johns et al. 1999; Belt et al., 2007). In Johns et al. (1999), a C_{25} diene was isolated in Antarctic sediment and Antarctic sea-ice diatoms and the diatom *Haslea ostrearia* were identified as sources in cultures.

1.3. Previous Work

Belt et al. (2007) proposed a biochemical proxy for sea-ice extent, termed IP_{25}. It is a highly branched monounsaturated isoprenoid with 25 carbons (Figure 1.4) and is biosynthesized by individual diatoms who live in/on sea ice. Even if the species is not specific to sea ice, individual organisms of that species who live on sea ice produce IP_{25}, whereas individuals of the same species who live in open water do not produce IP_{25}. Belt et al. (2007) isolated the IP_{25} molecule in samples of sea ice and surface sediments in the Canadian Arctic and applied it as a sea-ice presence indicator there.

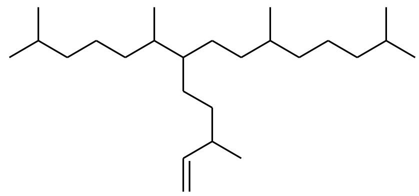

Figure 1.4. Chemical structure of IP_{25}

Samples of planktonic diatoms from open water in the Canadian Arctic were also analyzed for IP_{25} content, but no detectable amounts of IP_{25} were found, confirming the specificity of IP_{25} to sea ice and contributing to its usefulness and reliability as a sea-ice indicator. Another quality of a reliable sea-ice proxy is resistance to degradation. Although HBIs are subject to degradation, alkenes with three or more double bonds have been observed to degrade much faster in the environment compared to alkanes or alkenes with one or two double bonds (Barrick et al., 1980; Dunlop and Jefferies, 1985; reviewed by Rowland and Robson, 1990). Since IP_{25} has only one double bond, its resistance compared to other HBIs also contributes to its ability to be applied as a paleoenvironment proxy.

IP_{25} is used as a qualitative sea-ice proxy in several subsequent studies (Massé et al., 2008; Vare et al., 2009; Andrews et al., 2009; Müller et al., 2009). In Massé et al. (2008), relative abundances of IP_{25} were measured throughout a sediment core taken off the north coast of Iceland, representing the last 1000 yrs. The relative abundances of IP_{25}

were compared to historical records of sea ice and diatom-derived reconstructed sea surface temperatures for the same area and time. Higher abundances of IP_{25} were observed in sediments from the Little Ice Age, which also correspond to historic records of more intense sea-ice conditions and lower diatom-derived sea surface temperatures. Lower abundances of IP_{25} were observed in sediments from the Medieval Warm Period, which also correspond to historic records of less intense sea-ice conditions and higher sea surface temperatures.

Vare et al. (2009) reports an IP_{25} derived sea-ice reconstruction for the Barrow Strait in the Canadian Arctic Achipelago from 10.0-0.4 cal kyr BP. Relative IP_{25} abundances and IP_{25} fluxes were determined from a sediment core representing the aforementioned time interval. These data were compared to each other and to carbon isotope values of bulk organic matter from the same samples. Periods of higher IP_{25} abundances, higher IP_{25} fluxes and higher $\delta^{13}C$ values are interpreted as periods of more intense spring sea-ice conditions, while periods of lower IP_{25} abundances, lower IP_{25} fluxes and lower $\delta^{13}C$ values are interpreted as periods of less intense sea-ice conditions. The higher marine source organic matter has a higher $\delta^{13}C$ value ($-19^{o}/_{oo}$ to $-24^{o}/_{oo}$) compared to that of terrigenous source organic matter ($-26^{o}/_{oo}$ to $-28^{o}/_{oo}$). Thus, the higher $\delta^{13}C$ values are used to indicate more intense sea-ice conditions because at times of thicker and/or more extensive sea-ice coverage, a greater percentage of the bulk organic matter comes from marine sources, as less terrigenous organic matter can be deposited into Barrow Strait.

Andrews et al. (2009) presents a qualitative sea-ice record for the northwest Icelandic shelf and Denmark Strait over the last 2000 years based on relative IP_{25}

abundances from a marine sediment core. Müller et al. (2009) reports detecting IP_{25} in sediment as old as 30 kyrs, the earliest detected IP_{25} occurrence to date. Relative IP_{25} abundances from the sediment core are used to construct a qualitative sea-ice record in the Fram Strait for the last 30 kyrs.

1.4. Objectives

One objective of this study was to identify and quantify the highly branched isoprenoid, IP_{25}, in surface sediments from the Bering and Chukchi Seas. This was achieved by a series of analyses through which lipids are extracted from dried sediment, purified, and IP_{25} identified using gas chromatography and mass spectrometry (GC/MS).

The second objective was to determine if this molecule is a useful and reliable proxy for sea-ice presence/duration in these locations. This was achieved by comparing the measured IP_{25} concentrations with modern annual duration of sea ice.

1.5. Importance of Project

The effects of global warming are felt more dramatically in the polar regions than in the lower latitudes. Over the last few decades, average annual Arctic temperatures have risen at twice the rate as those of the rest of the world and as a result, sea-ice thickness and extent have been decreasing (Thomas and Dieckmann, 2003; Hassol, 2004,). In the Arctic over the past 30 years, the average sea-ice thickness has decreased by 10-15% and the average annual sea-ice extent has decreased by 8-10%, approximately equal to 1 million km^2. The average extent of summer sea-ice has decreased by 15-20% over the same period (Hassol, 2004; Johannessen et al., 1999; Meier et al., 2005). As temperatures on Earth continue to rise, loss of sea-ice extent may have a positive feedback effect on the climate, causing temperatures to increase even more rapidly (Vinnikov et al., 1999; Thomas and Dieckmann, 2003; Grebmeier et al., 2006). Knowing the southward extent and annual duration of Artic sea ice in the past and understanding its relationship with climate under different forcings, will aid in the investigation of how Earth's climate is changing now and will continue to change in the future. Currently, global and regional climate models can predict and reconstruct sea-ice cover only with very limited accuracy. If IP_{25} can be established as a reliable proxy for sea-ice duration, it can be applied down core and be used to test paleo sea-ice conditions constructed from climate models.

CHAPTER 2

INVESTIGATION OF IP_{25} AS A SEA-ICE DURATION PROXY

2.1. Introduction

In this study we show that the biomarker sea-ice indicator, IP_{25}, can be used as a quantitative proxy for average annual sea-ice duration. Belt et al. (2007) first presented the compound IP_{25} as a molecular proxy for sea-ice extent. Subsequent studies by Massé et al. (2008), Vare et al. (2009), Andrews et al. (2009), and Müller et al. (2009) have confirmed its usefulness as a qualitative proxy for sea-ice conditions. However, a connection between IP_{25} and a quantifiable amount of sea ice had not been reported previously. Here, IP_{25} was extracted from Bering and Chukchi Sea surface sediments and compared to mean annual sea-ice duration derived from satellite data, mean annual and August sea surface temperatures (SSTs), and mean annual and August sea surface salinities (SSSs). Our results show an exponential relationship between TOC-normalized IP_{25} concentration and months of sea ice/year (R^2=0.72, n=56), negative exponential relationships between IP_{25} concentration and average annual and August SSTs (R^2=0.67, n=53; R^2=0.81, n=53, respectively), and negative exponential relationships between IP_{25} concentrations and average annual and August SSSs (R^2=0.52, n=53; R^2=0.77, n=53, respectively). An exploratory study was also conducted to investigate whether solar insolation influences IP_{25} biosynthesis. An established calibration relating IP_{25} concentrations to months of sea ice/year would be invaluable to better understanding how changes in sea-ice duration affect and reflect changes in the global climate system.

2.2. Background

Seasonal sea ice has an intimate and complex relationship with global climate. This reflects the interplay between ice thickness, extent, and duration and the heat, moisture, and gas exchange between the ocean and atmosphere. Sea ice helps cool the atmosphere by reflecting incoming solar energy (Royer et al., 1990; Parkinson et al., 2001; Thomas and Dieckmann, 2003) and influences atmospheric circulation and pressure, storm intensity, and precipitation (Budikova, 2009). In the North Atlantic, sea-ice formation also contributes to global meridional ocean circulation by creating denser surface waters that sink and drive thermohaline circulation (Broecker, 1997, McBean et al., 2005). Sea ice also plays a critical role in high latitude marine carbon cycling. In ice covered seas, ice algae uptake carbon faster than pelagic phytoplankton (Lee et al., 2008). Organic matter shed from melting sea ice also provides a faster carbon burial mechanism (Riedel et al., 2006). The areal extent/duration of sea ice in the Arctic Ocean and its marginal seas through geologic time is valuable information for better understanding the relationship between sea ice and climate.

Indicators of sea ice preserved in marine sediments have proven useful in developing paleo sea-ice records. However, these approaches have been limited by poor preservation (e.g. diatom frustules; Barron, 1993) and sparse distribution (e.g. dropstones; Sakamoto et al., 2005). Belt et al. (2007) have proposed the compound IP_{25} as a promising molecular proxy for sea-ice extent. IP_{25} is a highly branched isoprenoid (HBI) monoene biosynthesized exclusively by diatoms, *Haslea spp*., associated with sea-ice. IP_{25} in marine cores has been used as a qualitiative indicator of sea ice off the northern coast of Iceland (Massé et al., 2008; Andrews et al., 2009), in the Fram Strait

(Müller et al., 2009) and in the Barrow Strait in the Canadian Arctic Archipelago (Vare et al., 2009). However, IP_{25} analysis has not previously been applied to sediments from the Bering and Chukchi Seas, nor has a quantitative association between IP_{25} and sea-ice duration been examined. This region represents a promising natural laboratory for developing a core-top calibration between sea ice and the IP_{25} biomarker because it exhibits a wide range of seasonal ice duration, with year-round open water in the southern Bering Sea, and perennial sea ice in the northern Chukchi Sea.

2.3. Methods

2.3.1. Sediment sampling

A van Veen grab was used to collect samples of surface sediment from across the Bering Sea on the *USCGC Healy* 0702 cruise in 2007 and across the Chukchi Sea on the *R/V Norseman II* cruise in 2008. Samples were frozen until analysis. A subset of 56 representative samples from the latitude gradient spanning 60° N to 72° N, with sea-ice durations ranging from 0 to 11 months of sea ice per year was analyzed (Figure 2.1).

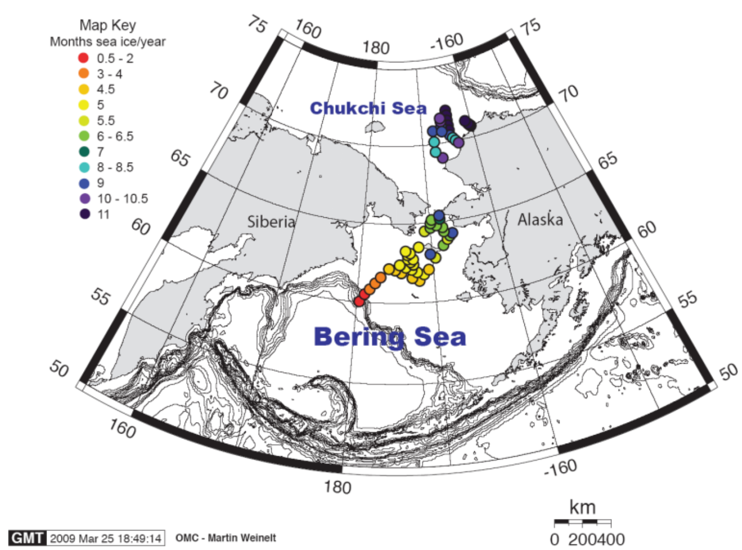

Figure 2.1. Sample site locations in the Bering and Chukchi Seas with colored circles denoting average annual duration of sea ice from 1979-1992.

2.3.2. Elemental Analysis

Seven microgram aliquots of dry sediment were measured into tin weighing boats and analyzed for total nitrogen content with a Costech ECS140 Elemental Analyzer (EA). Total organic carbon content was determined by a similar procedure, using silver weighing boats, and dissolving inorganic carbon in the samples with sulfurous acid prior to EA analysis. Acetanilide standards were analyzed with both sets of samples.

2.3.3. Lipid Purification and Analysis

Sediment samples were freeze-dried and homogenized. An internal standard (10μl of 10 μg/ml 7-hexyl nonadecane) was added to the dry sediment for quantification on a gas chromatograph and mass spectrometer (GC/MS). Lipids were extracted from the sediment samples with three rinses of 3 ml of 2:1 DCM:Methanol, which involved centrifuging each sediment sample with the solvent and removing the lipid extract in solvent by pipette. Two ml of methanol, 2 ml of hexane, and 1 ml of water were added to each dried lipid extract, shaking vigorously between each. The hydrocarbon bearing hexane fraction floated above the methanol and water layer which contained more polar compounds. The hexane layer was transferred from the top of each sample onto its own hexane conditioned silica gel column with three rinses of 2 ml of hexane, shaking vigorously between each rinse. Further purification of the hydrocarbon fraction was performed according to methods described in Belt et al. (2007). An Agilent 7890A gas chromatograph (GC) and 5975C mass spectrometer (MS) were used to perform GC/MS analysis of the final purified extract. The GC oven temperature was programmed to start at 40^{o}C, increase 10^{o}C/min until 300^{o}C and held at that final temperature for 10 min.

IP_{25} in samples was quantified using a ratio of the abundance of fragment ion m/z=350 from IP_{25} and fragment ion m/z=266 from the internal standard (7-hexyl nonadecane) as implemented in Belt et al. (2007), Massé et al. (2008), Vare et al. (2009). Each sample's total IP_{25} mass was then either divided by the mass of the dry sediment to calculate μg IP_{25}/g dry sediment, or by the mass of total organic carbon (TOC) in the original sediment sample to calculate μg IP_{25}/g TOC.

2.3.4. Sea-ice Satellite Data

IP_{25} concentrations produced by GC/MS analysis were compared to sea-ice duration data derived from the passive microwave satellite products: SSM/I and SMMR (Edwards, 1989; NASA, 1992; NSIDC, 1992; 1993). Satellite data of monthly sea-ice concentrations was averaged over the 13 year period from 1979-1992 using the "SEE_ICE" tool (Schweitzer, 1995). Monthly sea-ice concentrations within the dataset range from ice free (0% sea-ice concentration to completely ice covered (100% sea-ice concentration). Monthly sea-ice concentration was translated into months of sea ice per year using the method described in Armand et al. (2005).

2.3.5. SST and SSS data

Average annual and average August sea surface temperature and salinity data were obtained from the Levitus94 dataset. This dataset is oceanographic data from the National Oceanographic Data Center (NODC) archives collected from 1990-1992 (Levitus and Gelfeld, 1992) and is compiled with data gathered by the National Oceanographic Data Archaeology and Rescue (NODAR) and the IOC/IODE Global

Oceanographic Data Archaeology and Rescue (GODAR) (Levitus et al., 1994). The Levitus dataset was chosen because the years of data collection overlapped with those of the satellite-based sea-ice dataset.

2.3.6. Insolation and "bloom start date" data

Mean daily and monthly insolation data were obtained from *Insola*, an online program designed to solve astronomical computations of Earth's insolation from -250 million to +250 million years relative to the year 2000 (Laskar et al., 2004). *Insola*'s solution set, *La2004*, which has a sampling step of 100 years, was used to procure these data from year 2000, as this was the chronologically closest year to the time span of the sea-ice concentration data used in this study (1979-1992). More specifically, a mean daily insolation value for the approximate "bloom start date" at each site was obtained from this program and solution set. "Bloom start dates" for the end member sample sites (60^{o}N and 72^{o}N) were estimated from literature (Alexander and Niebauer, 1981; Lalande et al., 2007) and "bloom start dates" for the in-between sites along the latitudinal transect (60^{o}N-72^{o}N) were calculated using a linear equation ($y=4.2415x - 219.6$) that connects the end member date estimations (Figure 2.2).

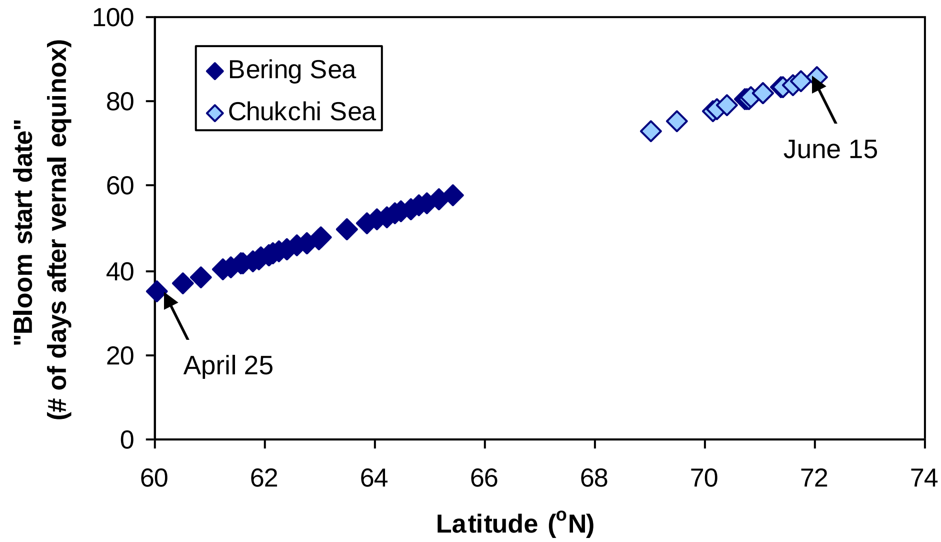

Figure 2.2. Graph of the linear equation, y=4.2415x – 219.6, used to estimate "bloom start dates" for sample sites in the Bering and Chukchi Seas; the "y-axis" is presented in number of days after the vernal equinox (i.e. 1^o=March 21, 2^o=March 22, and so forth)

Several assumptions were made in constructing this equation: 1) the ice algal bloom at 60^oN occurs on April 25; 2) the ice algal bloom progresses northward linearly; 3) the ice algal bloom at 72^oN occurs on June 15. Alexander and Niebauer (1981) report the ice algal bloom starting at the Bering Shelf slope (~60^oN) within the last two weeks of April, justifying the use of April 25 as a bloom start date in this study. A linear relationship between latitude and ice algal bloom initiation was chosen for simplicity. Lastly, Lalande et al. (2007) reports the ice algal bloom occurring in the Chukchi Sea in May/June with observations of sea-ice melting and algae blooming in mid-June at ~72^oN. Therefore June 15 was chosen for the northern Chukchi Sea (72^oN) bloom start date in this study. A "bloom month" was assigned to each sample site based on which month (April, May or June) the site's "bloom start date" fell in. The "bloom month" is considered in this study in order to best represent the mean monthly insolation values and sea-ice concentration during bloom time.

Mean monthly insolation (W/m^2) and mean monthly sea-ice concentration (0-100%) data were multiplied to produce a value, which considers each site's solar insolation and sea-ice concentration. This product, termed "insolation on sea ice" represents the mean amount of solar radiative energy received by the area of sea ice within a square meter of sea surface (W/m^2 * % sea ice). For example, if a site's mean June insolation is 473 W/m^2 and its mean June sea-ice concentration is 44%, it is assumed that 44% of every square meter of sea surface at that site is covered by sea ice and, therefore, an average 44% of the total 473 W/m^2, or 208.12 W/m^2 is received by sea ice at that site in June.

This "insolation on sea ice" is utilized in different ways in this study. The first is summing the mean monthly "insolation on sea ice" values for 1 year at each site. This considers each site's yearly changes in insolation and sea-ice concentration. Mean monthly "insolation on sea ice" for each site's "bloom month" is also used to evaluate the possible influence that bloom time insolation and sea-ice concentration have on IP_{25} synthesis.

2.4. Results and Discussion

2.4.1. Elemental Analysis

Total organic carbon (TOC) values range from 0.04 to 2.25 weight percent in the Bering Sea and 0.27 to 1.30 weight percent in the Chukchi Sea. C/N ratios range from 0.99 to 10.04 in the Bering Sea, although 40 of 41 of those samples have C/N ratios between 3.98 and 10.04. These values are approximately between 4 and 10, which indicate a marine carbon source (Meyers, 1994). In the Chukchi Sea, C/N ratios range from 6.63 and 11.81, although 15 of 16 of those samples have C/N ratios between 4 and 10. The sample from the Chukchi Sea that had a C/N ratio exceeding 10 is from relatively close to shore (12 km), but not the closest among our sample locations. However, this higher C/N ratio does not exceed 20, which would indicative a terrigenous carbon source (Meyers, 1994). It is likely that this sample location has a mixed carbon source.

2.4.2. IP_{25} and sea surface conditions

GC/MS analysis of lipid extracts reveals the presence of IP_{25} in all examined sediment samples. This is consistent with satellite observations of sea-ice coverage (1979-1992), which reveal that seasonal sea ice had been present at all the sample locations during that time span (Edwards, 1989; NASA, 1992; NSIDC, 1992; 1993). Average IP_{25} concentrations (μg IP_{25}/g dry sediment) from the Chukchi Sea sediment (range of 1.7 - 20.2 μg/g dry sediment) are 10 times greater than those from the Bering Sea sediment (range of 0.3 - 3.6 μg/g dry sediment) (Figure 2.3). The result of the Student T-test identifies a 1.7E-14% probability that the mean Bering and Chukchi Sea IP_{25} concentrations differ coincidently. Higher concentrations of IP_{25} correspond to the average longer duration of sea-ice per year in the Chukchi Sea (8-11 months/year) compared to that in the Bering Sea (0.5-9 months/year). These data suggest an exponential relationship between IP_{25} concentration (μg IP_{25}/g dry sediment) and months of sea-ice/year (R^2=0.43, n=56).

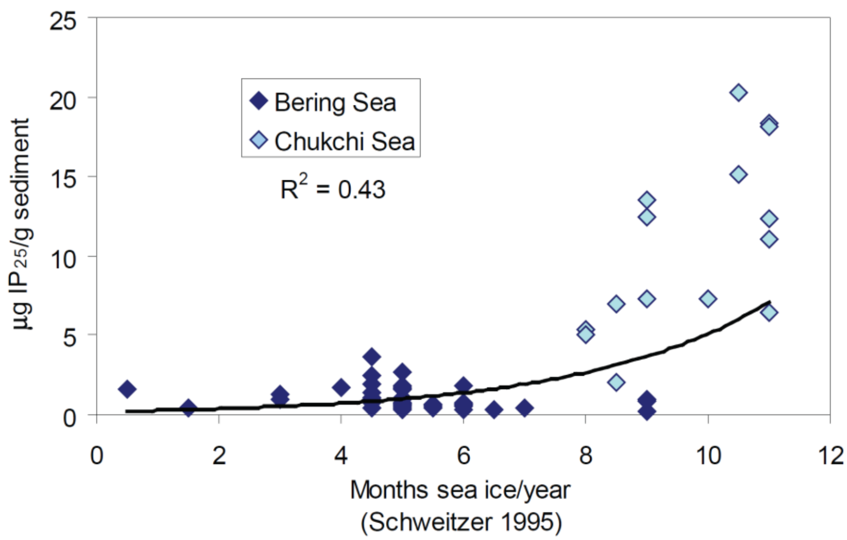

Figure 2.3. IP_{25} concentrations in the Bering and Chukchi Seas, compared to average annual sea-ice duration, R^2=0.43, n=56

One explanation for this relationship is that ice algae may produce more IP_{25} to adapt to living under more intense sea-ice conditions. Although little is known about the physiological purpose of IP_{25}, further research may reveal an adaptive relationship between IP_{25} biosynthesis and sea-ice conditions, similar to that between alkenone biosynthesis by coccolithophorid phytoplankton and growth temperature (Brassel et al., 1986).

An alternate explanation is that springtime insolation influences biosynthesis of IP_{25}. Sea-ice algae biosynthesize a greater amount of lipids when more sunlight (greater intensity and more hours of sunlight) is available at the time they bloom (Smith et al., 1987). The ice algal bloom starts at the southern Bering Sea ice-edge in March/April and progresses northward into the Chukchi Sea as the ice-edge retreats through May/June (Rho and Whitledge, 2007; Wang et al., 2005). Because the Chukchi Sea ice algae bloom later in the spring, more daily insolation is available to ice algae there (~480 W/m^2) than to those in the Bering Sea (~390 W/m^2) at the time of their respective blooms. Therefore, ice algae in the Chukchi Sea may be able to biosynthesize a greater mass of IP_{25} because they have access to more sunlight at the time of their bloom.

A third explanation for higher IP_{25} concentrations (μg/g dry sediment) in the Chukchi Sea is a greater amount of total organic matter input into the Chukchi compared to the Bering Sea. Our data show an approximate 15% higher mean TOC value in the Chukchi compared to that in the Bering Sea. Therefore, evaluating IP_{25} concentrations normalized to TOC (μg IP_{25}/g TOC) serves to more accurately represent relative IP_{25} concentrations in this study.

TOC-normalized IP_{25} concentrations increase exponentially with decreasing mean annual sea surface temperature (R^2=0.67, n=53, Figure 2.4). A similar relationship exists with mean August sea surface temperature (R^2=0.81, n=53, Figure 2.5). There are 53 data points because SST and SSS data were not available for all sites. It is not surprising that higher concentrations of IP_{25} are detected in areas with lower mean annual SSTs, as SST and sea-ice duration are not independent variables. Hence, it is also reasonable to observe a similar relationship between IP_{25} concentrations and mean August SSTs. Colder sea surface temperatures support higher concentrations of ice, thicker sea-ice formation and longer sea-ice duration (de Vernal and Hillaire-Marcel, 2000; Kunz-Pirrung et al., 2004). The regression between IP_{25} concentration and mean August SST has a higher correlation coefficient, compared to that of the regression with mean annual SST.

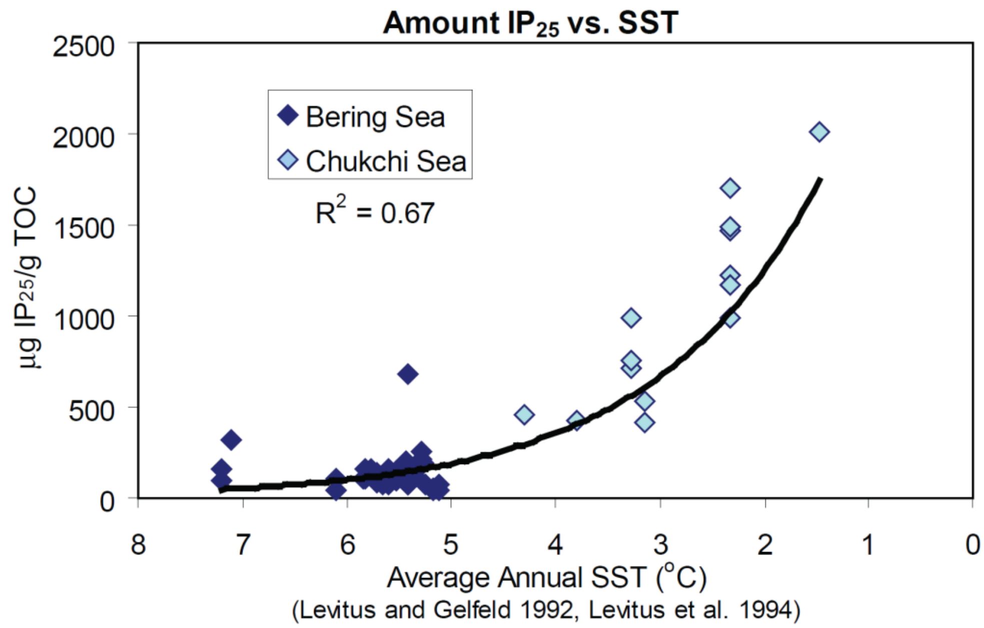

Figure 2.4. Negative exponential relationship between TOC normalized IP_{25} concentrations and average annual sea surface temperature in the Bering and Chukchi Seas, R^2=0.67, n=53 (Note reversed x-axis).

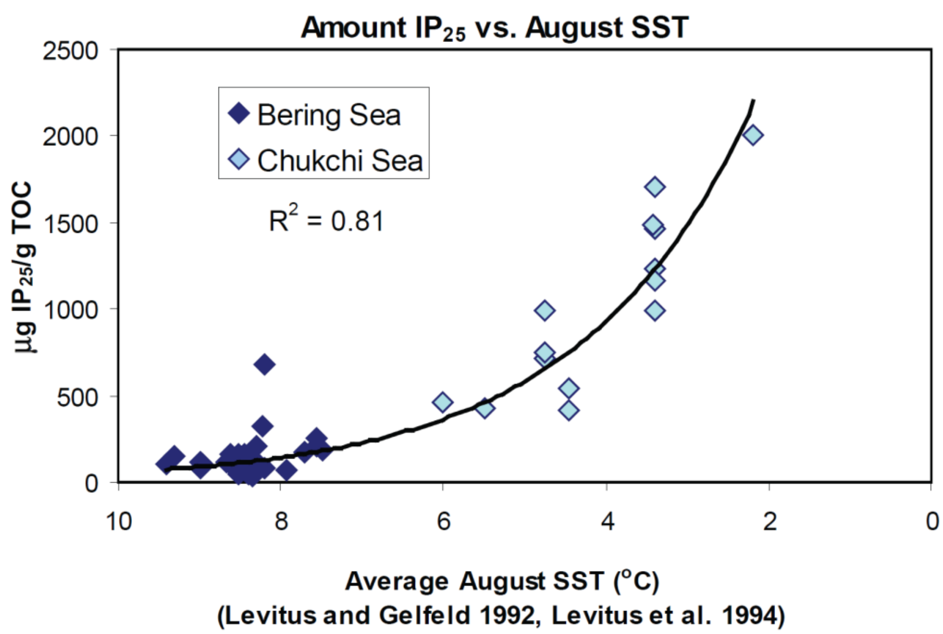

Figure 2.5. Negative exponential relationship between TOC normalized IP_{25} concentrations and average August sea surface temperature in the Bering and Chukchi Seas, R^2=0.81, n=53 (Note reversed x-axis).

TOC-normalized IP_{25} concentrations decrease exponentially with increasing mean annual sea surface salinity (R^2=0.52, n=53, Figure 2.6). A similar relationship also exists with mean August sea surface salinity (R^2=0.77, n=53, Figure 2.7). It is unclear whether SSS influences the biosynthesis of IP_{25} or if this relationship reflects the interconnectedness of sea-ice duration, SST and SSS. De Vernal et al. (2004) reconstructed LGM annual sea-ice duration, and August sea surface temperature and salinity using a modern calibration of dinocyst assemblages from 940 sites across the Arctic. The authors note high sea-ice duration during the LGM accompanied by low August SSTs and low August SSSs. The low August SSSs during the LGM are attributed to dilution from summer melting of continental ice sheets and sea-ice. These data agree with the sea surface condition relationships observed in this study. As seen with the SST data, the correlation coefficient of the regression between IP_{25} concentration and mean August SSS is higher than that of the regression with mean annual SSS.

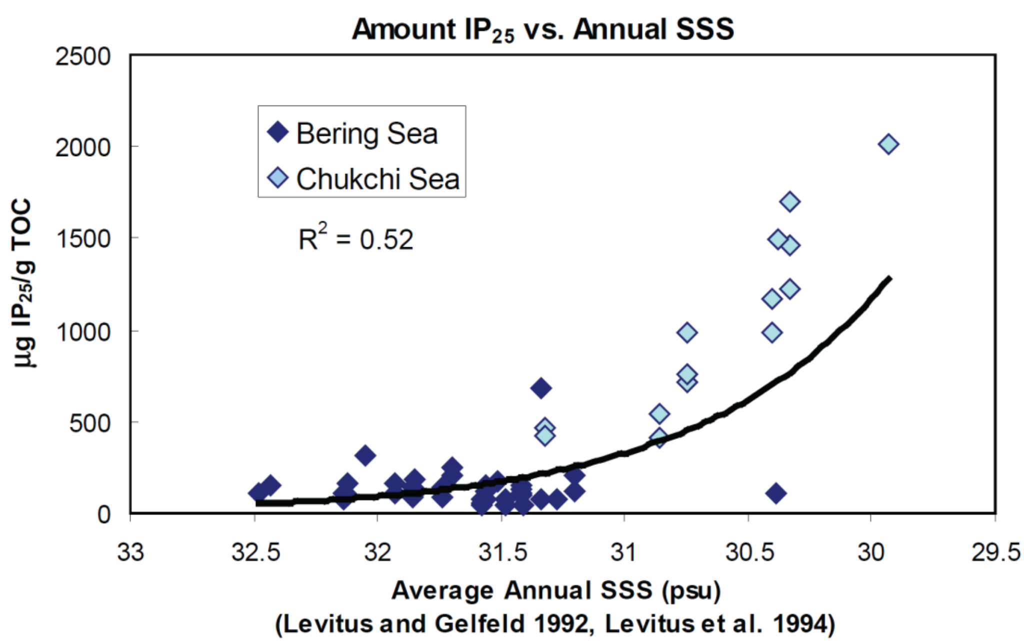

Figure 2.6. Negative exponential relationship between TOC normalized IP_{25} concentrations and average annual sea surface salinity in the Bering and Chukchi Seas, R^2=0.52, n=53 (Note reversed x-axis)

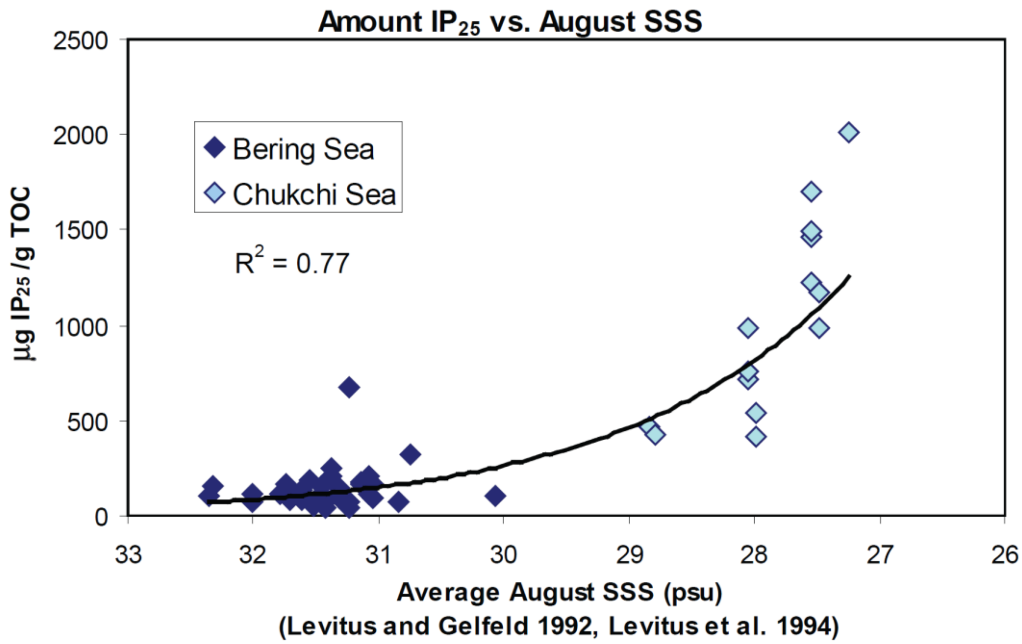

Figure 2.7. Negative exponential relationship between TOC normalized IP_{25} concentrations and average August sea surface salinity in the Bering and Chukchi Seas R^2=0.77, n=53 (Note reversed x-axis)

TOC-normalized IP_{25} concentrations also increase exponentially with increasing annual sea-ice duration (R^2=0.72, n = 56, Figure 2.8). The equation for this curve is $y=19.284e^{0.3637x}$, where x= months of sea ice/year and y= µg IP_{25}/g TOC. The correlation coefficient for this relationship (R^2=0.72) is higher than that for the regression between IP_{25} concentration (µg/g dry sediment) and sea-ice duration (R^2=0.43), and either of the regressions between TOC-normalized IP_{25} concentration and mean annual SST and SSS. However, the regressions with the highest correlation coefficients exist between TOC-normalized IP_{25} concentration and average August sea surface temperature and salinity. This suggests that IP_{25} concentrations may more accurately record fall sea surface conditions, rather than mean annual, which is surprising. Although the regression between TOC-normalized IP_{25} concentrations and annual sea-ice duration may not have the strongest correlation among these data, the usefulness of IP_{25} as a proxy for sea-ice presence and annual duration is not negated. IP_{25} is biosynthesized exclusively by diatoms that live in/on sea ice and, hence, sea ice is expected to influence IP_{25} production in some way (Belt et al., 2007).

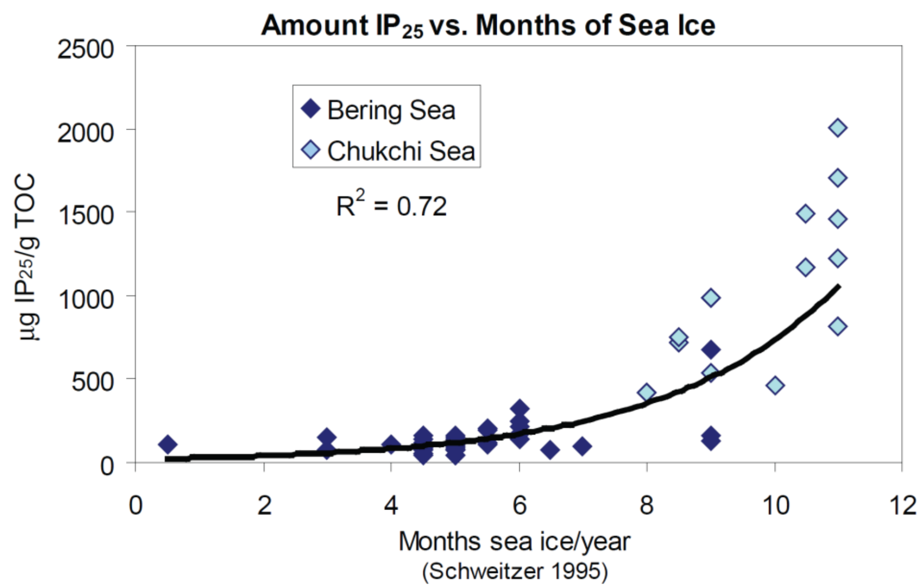

Figure 2.8. Exponential relationship between TOC normalized IP_{25} concentrations and average annual sea-ice duration in the Bering and Chukchi Seas, R^2=0.72, *n* = 56

2.4.3. IP_{25}, insolation and sea-ice conditions

Investigating the potential influence of solar insolation on IP_{25} biosynthesis was motivated by the knowledge that the Bering and Chukchi Sea ice algal bloom progresses northward, following the sea-ice edge as it recedes in the spring (Alexander and Niebauer, 1981), and that lipid production in sea-ice algae increases with increased solar insolation (Smith et al., 1987). The mean daily insolation on an estimated "bloom start date," described in the Methods section, is utilized here to investigate if the amount of insolation that ice algae receive when they bloom influences the amount of IP_{25} the algae biosynthesize. The result shows that TOC-normalized IP_{25} concentrations increase exponentially with increasing mean daily insolation at the time of algal bloom (R^2=0.80, n=56, Figure 2.9). In the Bering Sea there is a gradual increase in IP_{25} concentrations from 350-425 W/m^2 and a much steeper increase in IP_{25} concentrations in the Chukchi Sea from 470-500 W/m^2. Between 425 W/m^2 and 470 W/m^2, there is a threshold which marks the shift from a gradual to a steeper increase in IP_{25} concentrations. This suggests that sea-ice diatoms respond to increased bloom time insolation by producing greater amounts of IP_{25} and that there may be a threshold around 450 W/m^2 at which they respond by producing exponentially increased amounts of IP_{25}.

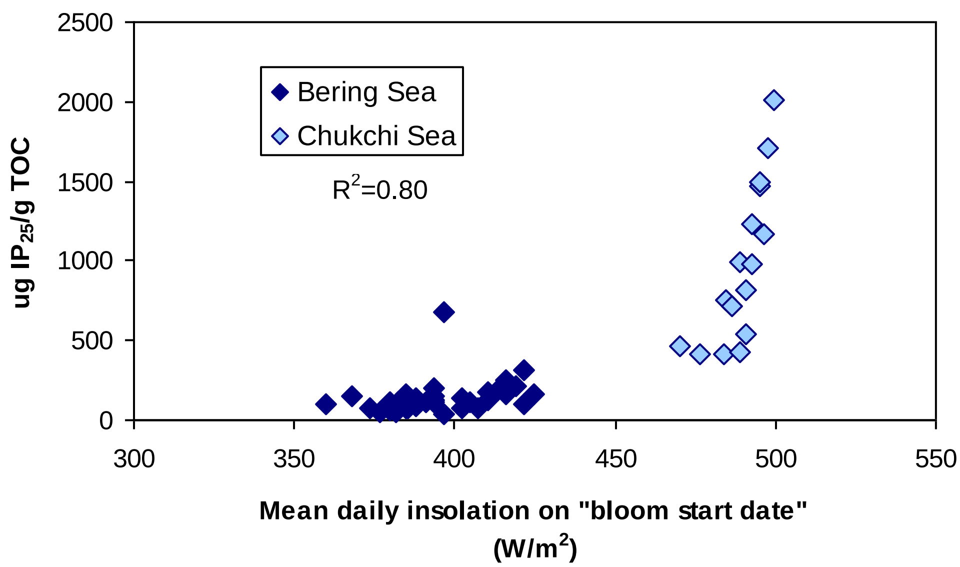

Figure 2.9. Exponential relationship between TOC-normalized IP_{25} concentrations and mean daily insolation on “bloom start date” in the Bering and Chukchi Seas, R^2=0.80, n=56

However, Belt et al. (2007) reports the absence of IP_{25} in samples from year round ice-free seas, and the ubiquitous presence of IP_{25} in samples from seas that contain seasonal sea ice. Insolation may influence IP_{25} production, but not insolation alone. Because IP_{25} production is specific to sea-ice diatoms (Belt et al. 2007), sea-ice conditions are expected to have a role in it as well. “Insolation on sea ice,” described in the Methods section, is a calculation to account for a site's sea-ice concentration and insolation. TOC-normalized IP_{25} concentrations increase exponentially with the sum of one year's mean monthly "insolation on sea ice" (R^2=0.77, n=56, Figure 2.10).

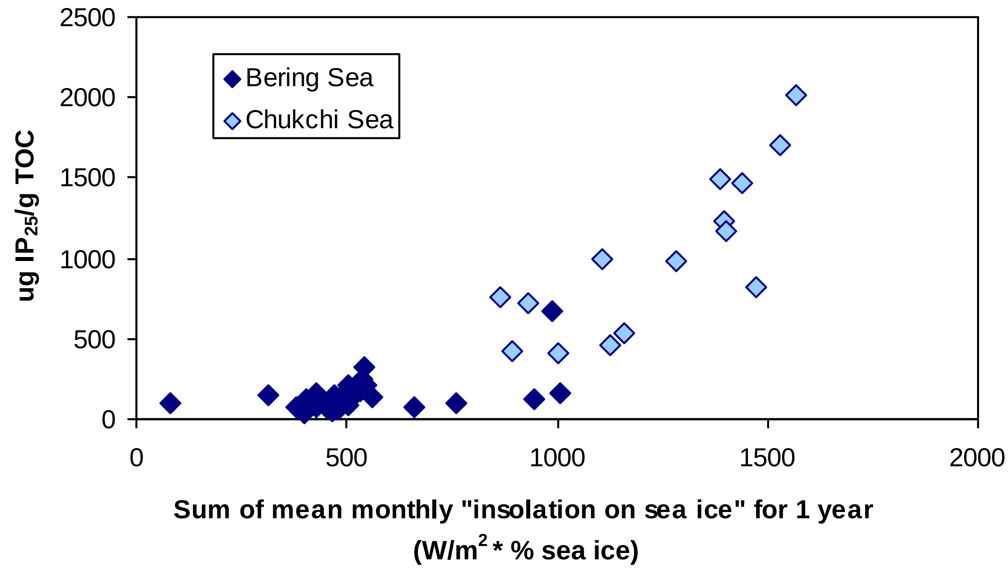

Figure 2.10. Exponential relationship between TOC normalized IP_{25} concentrations and sum of mean monthly "insolation on sea ice" in Bering and Chukchi Seas, R^2=0.77, n=56

Mean bloom month "insolation on sea ice," that is, mean monthly "insolation on sea ice" for the month in which the bloom occurs at a given site, is also compared to IP_{25} concentration. TOC-normalized IP_{25} concentrations increase exponentially with increasing mean bloom month "insolation on sea ice" (R^2=0.78, n=56, Figure 2.11). Both graphs (Figure 2.10 and Figure 2.11) show similar results. The regressions between IP_{25} concentrations and either set of "insolation on sea ice" values are stronger than the regression between IP_{25} concentration and mean annual sea-ice duration alone (R^2=0.71, n=56, Figure 2.8). This suggests that IP_{25} production is influenced by insolation in addition to sea-ice concentration/duration.

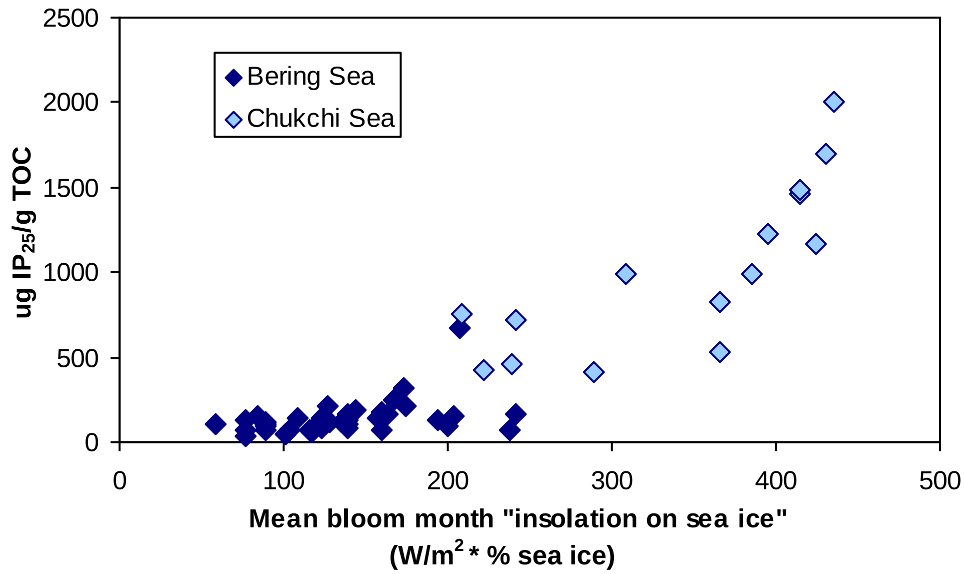

Figure 2.11. Exponential relationship between TOC-normalized IP_{25} concentrations and mean bloom month "insolation on sea ice" in the Bering and Chukchi Seas, R^2=0.78, n=56

2.5. Conclusions and Implications

IP_{25} was detected in all surface sediments from the Bering and Chukchi seas that had experienced at least an average 0.5 month of sea ice annually between 1979 and 1992. Average IP_{25} concentrations are higher in the Chukchi Sea compared to those in the Bering Sea. This corresponds with the longer average annual sea-ice duration and greater bloom time insolation in the Chukchi Sea compared to those in the Bering Sea. Moreover, an exponential relationship between TOC-normalized IP_{25} concentration and average annual duration of sea ice has been observed. Negative exponential relationships have been observed between IP_{25} and other sea surface conditions: average annual and August sea surface temperature and average annual and August sea surface salinity. Exponential relationships have also been identified between TOC-normalized IP_{25} concentrations and bloom time insolation and "insolation on sea ice." Future research will serve to better strengthen or define these exact relationships.

Reconstruction of paleo sea-ice duration in the Arctic Ocean and its marginal seas through geologic time is a valuable resource for climatology. More detailed records of paleo sea-ice extent and duration allow for a better understanding of the role sea ice plays in the global climate system. Specifically, long-term sea-ice records are needed to validate GCM outputs of earlier time slices, such as the LGM or Holocene Thermal Maximum, or as realistic boundary conditions for maximum/minimum ice extent. Records of sea-ice conditions in the Bering and Chukchi Seas are especially useful as there are fewer sea-ice and paleoclimate models focused in the North Pacific compared to in the North Atlantic and Antarctic.

IP_{25} is a viable proxy for paleo sea-ice duration in the Bering and Chukchi Seas. For this purpose, we propose the initial calibration equation of $y=1.9727\mathrm{Ln}(x)-4.017$ (the reciprocal of the exponential function identified earlier in this paper), where $x=\mu g\ IP_{25}/g$ TOC and y=months of sea ice/year. IP_{25} has previously been detected in sea ice and sediment samples from the Canadian Arctic (Belt et al., 2007; 2008; Vare et al., 2009) and in sediment samples from the North Icelandic Shelf (Massé et al., 2008; Andrews et al., 2009) and from the Fram Strait (Müller et al., 2009). Because IP_{25} has a circum-Arctic presence further regional calibrations and perhaps an Arctic-wide calibration for sea-ice duration should be explored. As for the temporal range of IP_{25}, Müller et al. (2009) show that IP_{25} is preserved in sediments as old as 30 cal. kyrs BP. There is little doubt that IP_{25} will be found in older sediments, however only analysis of such sediments will confirm this.

CHAPTER 3

PROPOSED FURTHER IP_{25}-RELATED RESEARCH

3.1. Introduction

This study identified relationships between TOC-normalized IP_{25} concentration in Bering and Chukchi Sea surface sediments and average annual duration of sea ice, average annual and August sea surface temperature and salinity, and bloom time insolation. With more time and resources, additional knowledge can be gained through further research and analyses of these samples. Further research will lead to the refinement of the regressions between IP_{25} and sea surface conditions, particularly average annual sea-ice duration, as well as to the establishment of downcore IP_{25} records in the Bering and Chukchi Seas. Comparing IP_{25} concentrations to other environmental conditions will also lead to a better understanding of what specific environmental factors influence IP_{25} production in sea-ice diatoms, hence which of these factors IP_{25} records in the sediment record, and perhaps what physiological role IP_{25} plays within the diatoms.

3.2. Surface Sediment Samples

Fifty-six Bering and Chukchi Sea surface sediment samples, chosen from an available total of 125 samples to represent the range of latitudes (60^{o}N-72^{o}N) and annual durations of sea-ice cover (0.5-11 months/year) were analyzed in this study. Analyzing as many of these samples as possible is advantageous to refining the exponential relationship between TOC-normalized IP_{25} concentration and annual duration of sea ice, as well as the relationships with sea surface temperature (SST) and salinity (SSS). More data may be able to increase correlation coefficients or better define correlation equations between TOC-normalized IP_{25} concentration and these sea surface conditions.

3.3. Sediment Core Samples

This study focused on IP_{25} analysis of surface sediments and comparing these concentrations with modern annual sea-ice duration. However, there are sediment cores that had been collected from the Bering and Chukchi Seas on the *USCGC Healy* 2002 cruise that may be available for downcore IP_{25} analysis. A few Bering Sea cores have been suggested for IP_{25} analysis because some previous work has already been conducted on them (correspondence with Beth Caissie). These are 3JPC, 17JPC, and 51JPC (for additional information on these cores, please see Appendix A). Additional cores from the Bering Sea will become available in December 2010 from the Integrated Ocean Drilling Project (IODP) Expedition 323 (Expedition 323 Scientists, 2010). These cores have bottom ages ranging from 0.5-4 Ma making them valuable for investigating the presence of IP_{25} in much older sediments. To date, the oldest sediments investigated are from 30 kyr B.P. (Müller et al., 2009). No downcore records of IP_{25} in the Bering and Chukchi Seas have been published; therefore analysis of available cores would allow for the construction of an IP_{25}-derived qualitative sea-ice record in these seas. Using our equation for sea-ice duration from known concentrations of TOC-normalized IP_{25} can then be applied and tested downcore to construct an IP_{25}-derived quantitative sea-ice record in the area.

3.4. Alkenones for $U^{k'}_{37}$

Several Bering Sea sediment samples were randomly selected for alkenone concentration analysis. A total lipid extract (TLE) was extracted from each sediment sample with a mixture of dichloromethane and methanol (9:1 v/v) by means of an accelerated solvent extractor. The TLE was dried down under nitrogen and dissolved in hexane. The hexane was transferred to a silica gel column and Fraction 1 was eluted with 4 mL of hexane. The vial that had contained the original TLE was rinsed with DCM and the DCM was transferred to the top of the same silica gel column. Fraction 2 was eluted with 4 mL of DCM. This Fraction 2 was expected to contain the alkenones. However, no detectable amounts of alkenones were found in these samples following gas chromatograph flame ionization detection (GC/FID) analysis.

This was surprising because alkenones have been found in sediments from the Bering Sea in other studies. Harada et al. (2003) detected alkenones in surface water and surface sediment samples from the eastern Bering Sea collected in 2000. Alkenone concentrations ranged from 0.109-1.42 μg/g in surface sediment samples and $U^{K'}_{37}$ temperature estimates from these alkenone concentrations matched observed September sea surface temperatures in the area. In that study, TLE samples were saponified in 0.5-mol/L KOH in methanol. The neutral fraction was recovered with a pipette in hexane and transferred to a silica gel column. Fraction 1 was eluted with hexane and Fraction 2 was eluted with a hexane/toluene mixture followed by a hexane/ethyl acetate mixture. Fraction 3 contained the alkenones and was eluted from the column using two hexane/ethyl acetate mixtures (the first was 85:15 v/v; the second was 4:1 v/v). Saponification does not affect alkenone identification/detection, so not saponifying TLE samples in my study is not the discrepancy. Ethyl acetate is a more polar solvent than dichloromethane, so perhaps that is why Harada et al. (2003) were able to detect alkenones in their Fraction 3 whereas I could not in my Fraction 2.

Caissie et al. (2010) were also able to detect alkenones in surface sediment and sediment core samples from the Bering Sea. Like Harada et al. (2003), $U^{K'}_{37}$ temperature estimates from surface sediments matched current average summer sea surface temperatures. The alkenone analysis procedure from Herbert and Schuffert (1998) was followed, which involves running the whole TLE in toluene on GC/FID without any column chromatography beforehand.

3.5. Glycerol Dialkyl Glycerol Tetraethers for TEX_{86}

Several Bering Sea samples were randomly selected for glycerol dialkyl glycerol tetraether (GDGT) analysis. A total lipid extract (TLE) was extracted from each sediment sample with a mixture of dichloromethane and methanol (9:1 v/v) by means of an accelerated solvent extractor. The TLE was analyzed for GDGT content by high performance liquid chromatography and mass spectrometry (HPLC/MS). No detectable amounts of GDGTs could be identified in the samples.

Schouten et al. (2002) report the presence of GDGTs in 40 surface sediments taken from around the world, including one from Skan Bay, located on the Bering Sea side of the Aleutian Islands. The GDGTs used in the TEX_{86} proxy have been detected in recent sediments from other polar seas such as around Antarctica, Canada, and the North Sea (Schouten et al., 2000; 2002). Kim et al. (2008) also report detecting GDGTs in surface sediment samples from the Arctic and Southern Oceans. These studies show that archaea in relatively colder waters produce GDGTs, but it is unclear why they were not detected in the Bering/Chukchi Sea surface sediments analyzed in this study.

Variable sample preparation and/or analysis may explain why GDGTs were not detected in our samples. Several TEX_{86} studies use soxhlet (Sinninghe-Damsté et al., 2002; Wuchter et al., 2006) or ultrasonication (Schouten et al., 2000; 2002; Wuchter et al., 2004) extraction to acquire TLE from sediment/particulates, however, Schouten et al. (2007) compared GDGT content of TLEs extracted by three different methods and detected negligible differences among soxhlet, ultrasonication, and accelerated solvent extractor extraction techniques.

Most of these studies (Schouten e al., 2002; Sinninghe-Damsté et al., 2002; Wuchter et al., 2004; 2006) also utilize a multiple step TLE purification process which involves running the TLE through an Al_2O_3 column and later filtering the resulting fraction through a Teflon filter, before analysis by high performance liquid chromatography/atmospheric pressure positive ion chemical ionization mass spectrometry (HPLC/APCI-MS). Perhaps purification of our Bering/Chukchi Sea sediments is necessary for GDGT detection. As for sediment sample mass, Schouten et al. (2000) reports detecting GDGTs from 1-5 g dry sediment sample masses, even from colder waters. Dry sediment sample masses analyzed in our study were within this range or greater, therefore it is unlikely that too small sample mass is the problem, unless these sediments truly contain undetectable amounts of GDGTs.

3.6. IP_{25} Synthesis and Insolation

The potential influence of solar insolation on IP_{25} synthesis was explored and discussed briefly in Chapter 2, however, further investigation is needed. IP_{25} is specific to sea-ice associated diatoms (Belt et al., 2007), therefore any role insolation plays on IP_{25}

synthesis is coupled with sea-ice conditions. The best method for evaluating how IP_{25} concentrations relate to insolation alone or insolation coupled with sea-ice conditions has not been identified, but several different approaches can be taken. Two methods used in this study, in addition to those described in Chapter 2, are presented here.

IP_{25} was plotted against a parameter called "ice hours" in this study. "Ice hours" is a term used to describe the product of hours of sunlight/month and monthly sea-ice concentration (0-100%), integrated over a year for a specific sample location. Sunlight data from the year 1985 was selected because 1985 is in the middle of the 1979-1992 sea-ice concentration data from Schweitzer (1995) utilized in this study. For more information about how "ice hours" values were calculated, please see Appendix B. This was an attempt to compare IP_{25} concentrations against some parameter that included sunlight availability and sea-ice conditions. The preliminary results are shown in Figure 3.1, but further analysis was abandoned after no apparent relationship was observed.

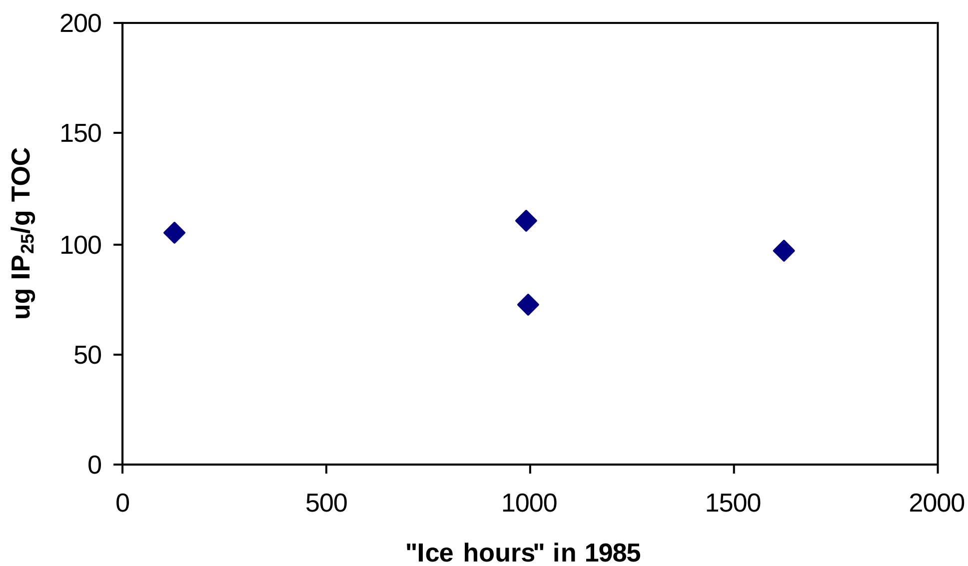

Figure 3.1. TOC-normalized IP_{25} concentrations plotted against "Ice hours," the product of hours of sunlight/month and monthly sea-ice concentration integrated over a year.

IP_{25} concentrations were also plotted against "hours of sunlight per day at time of bloom." This pursuit was based on the knowledge that the Bering and Chukchi Sea-ice algal bloom progresses northward, following the sea-ice edge as it recedes in the spring (Alexander and Niebauer, 1981) and that lipid production in sea-ice algae increases with increased solar insolation (Smith et al., 1987). An equation was written to estimate the time of bloom along the latitudinal transect (60^{o}N-72^{o}N) from which these Bering/Chukchi Sea sediment samples represent (Figure 3.2). Several assumptions were made in constructing this equation: 1) the ice algal bloom at 60^{o}N occurs on April 25; 2) the ice algal bloom progresses northward linearly; 3) the ice algal bloom at 72^{o}N occurs on June 22. Alexander and Niebauer (1981) report the ice algal bloom starting at the Bering Shelf slope (~60^{o}N) in late April/early May, justifying the use of April 25 as a bloom start date in this study. A linear relationship between latitude and ice algal bloom timing was chosen for simplicity. Lastly, Lalande et al. (2007) reports the ice algal bloom occurring in the Chukchi Sea in May/June, therefore a mid/late-June date was chosen for the northern Chukchi Sea (72^{o}N) bloom time in this study. This same approach was used in the calculation of the equation to estimate "bloom start date" for data presented in Chapter 2. However, the equation presented here in Figure 3.2 was reevaluated and refined to produce a more reasonable estimate of "bloom start date" as presented in Figure 2.2. Only one change was made after reevaluation of the literature (Lalande et al., 2007): the 72^{o}N sample site's "bloom start date" was changed from June 22 to June 15.

Hours of sunlight for the 'bloom day' corresponding to each sample's latitude were acquired from the website of the United States Naval Oceanography portal (Internet

Reference 1) and were plotted against TOC-normalized IP_{25} concentrations. Springtime sunlight data were not available for sites in the Chukchi Sea because the "sun [is] above [the] horizon for [an] extended period of time" (Internet Reference 1). The results, shown in Figure 3.3, suggest that increased solar insolation at time of bloom may play a role in increased IP_{25} production in sea-ice algae in the Bering Sea.

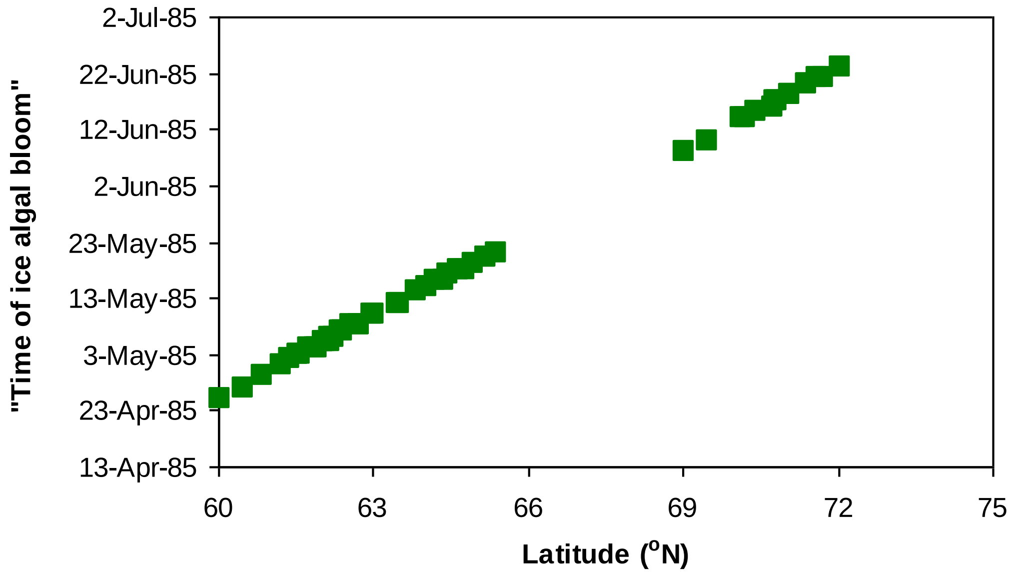

Figure 3.2. This graph represents the constructed equation, y=4.89x+30869, which related latitude to an approximate ice algal bloom time.

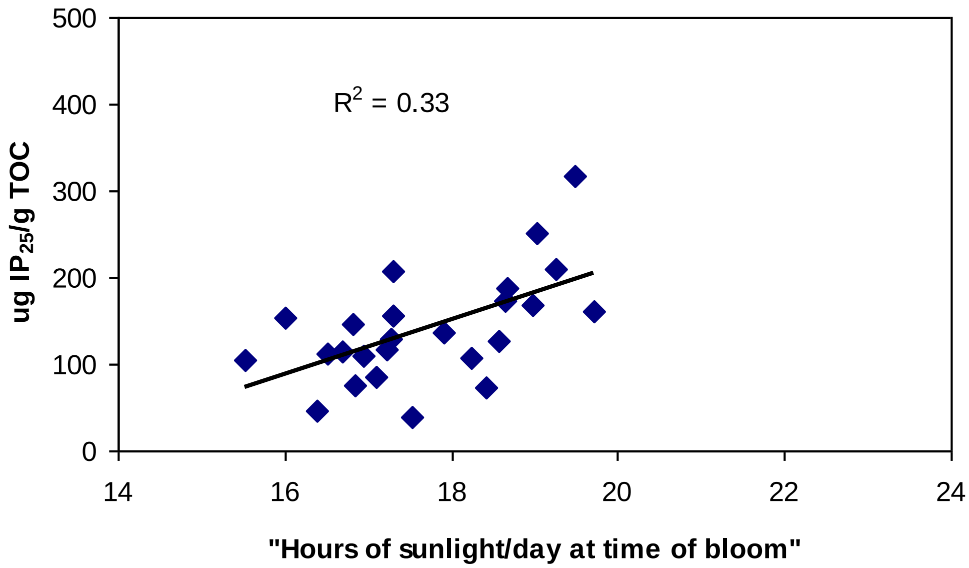

Figure 3.3. This graph suggests that Bering Sea ice algae may produce more IP_{25} when they bloom at times of increased hours of sunlight per day. R^2=0.33, n=25.

A fourth assumption, that sample locations between and including 71.4°N-71.7°N receive 24 hours of sunlight in mid-June, was made in an attempt to investigate if the increasing trend in the Bering Sea (Figure 3.3) continues into the Chukchi Sea. The results (shown in Figure 3.4) further support the suggestion that increased hours of sunlight per day at bloom time may influence the production of greater amounts of IP_{25} in sea-ice algae. These results also suggest that this relationship may be exponential, represented by the equation, $y=0.26e^{0.35x}$, where y=TOC-normalized IP_{25} concentration and x=hours of sunlight/day at bloom time (R^2=0.81, n=29).

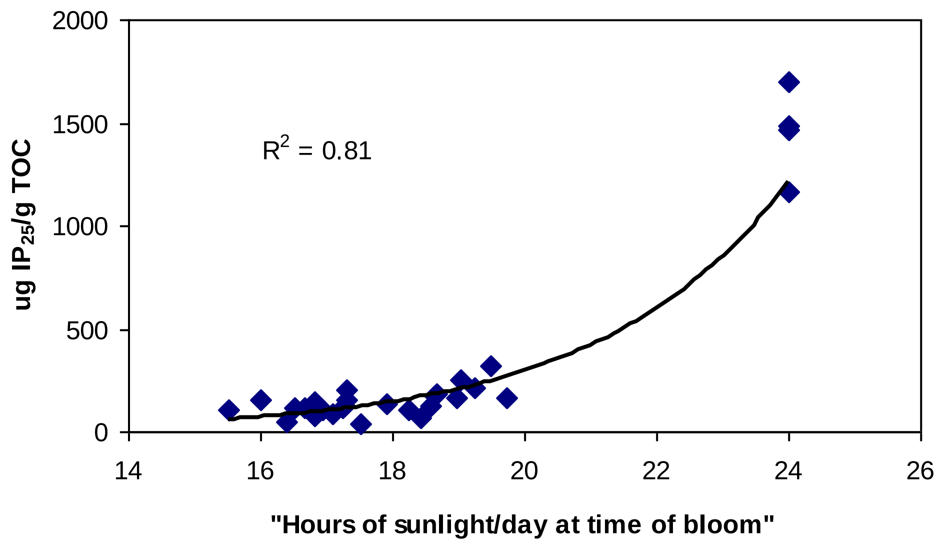

Figure 3.4. Possible exponential relationship between IP_{25} concentration and hours of sunlight/day at time of bloom, $y=0.26e^{0.35x}$, $R^2=0.81$, n=29.

3.7. IP_{25} Synthesis and Other Sea Surface Conditions

In this study, IP_{25} concentrations in surface sediments were plotted against mean annual sea-ice duration, sea surface temperature, and salinity. The role of solar insolation on IP_{25} biosynthesis had also started to be investigated. However, there are still more environmental factors, especially sea surface nutrient concentration and sea-ice thickness, which may exhibit a relationship to IP_{25} concentrations detected in underlying sediment.

Although several studies have identified light as the major controlling factor in high latitude bloom intensity and timing and overall growth of sea-ice algae (Meguro et al., 1967; Horner and Schrader, 1982; Niebauer et al., 1990), nutrient availability also affects primary production as well as the lipid composition of sea-ice algae (McConville, 1985). While increased nutrient concentrations (i.e. nitrate, phosphate, silica) enhance ice algal primary productivity, decreased concentrations of nutrients, particularly nitrogen, enhance ice algal lipid synthesis at the expense of proteins (Smith et al., 1987;

1997; Palmisano et al., 1988; Gradinger, 2009). Moreover, ice algae synthesize increasing amounts of neutral lipids (storage lipids) and decreasing amounts of structural/membrane lipids with nutrient depletion (Smith et al., 1997).

Sea surface nutrients may influence the biosynthesis of IP_{25}, which can be investigated by plotting IP_{25} concentrations against spring/summer sea surface nutrient concentrations. The Bering Sea ice edge bloom receives most of its sustaining nutrients from the upwelling nutrient-rich deep waters of the Bering Sea basin (Alexander and Niebauer, 1981; Niebauer et al., 1995). These waters upwell at the Bering Sea shelf break and the bloom benefits most from this nutrient source in colder years when the ice edge extends past the break (Alexander and Niebauer, 1981). Nutrient concentrations are highest at the ice edge in early spring but decrease through the season and northward as the bloom advances poleward with the receding ice edge (Alexander and Niebauer, 1981; Niebauer et al., 1995). This northward decrease in nutrient concentration accompanied by the observed northward increase in IP_{25} concentration in the Bering Sea (this study) seems to match the nutrient depletion/lipid synthesis enhancement relationship described in the literature, but more research is needed to confirm or deny this.

Maximum winter or mean annual sea-ice thickness may also influence IP_{25} production. Massé et al. (2008) and Vare et al. (2009) demonstrate that higher concentrations of IP_{25} indicate more intense sea-ice conditions, which include longer durations of and thicker sea ice. Plotting IP_{25} concentrations against any possible quantifiable feature of sea ice is necessary to better understand what most influences IP_{25} biosynthesis and thus what may drive fluctuations in IP_{25} concentrations. There may be a relationship between IP_{25} concentrations and maximum and/or mean annual sea-ice thickness. Sea-ice thickness affects under-ice irradiance, which together, may influence IP_{25} production by ice algae. Comparing IP_{25} concentrations to mean annual or seasonal under-ice irradiance might be useful as well.

3.8. Conclusions

There is still much work, IP_{25}-related and otherwise, that can be done on these Bering and Chukchi Sea surface sediment samples and any available sediment cores from these areas. IP_{25} regressions can be refined and correlation equations better defined. Downcore IP_{25} records can be established in the Bering and Chukchi Seas as well. IP_{25} concentrations are related to average annual sea-ice duration, sea surface temperature and salinity in this study; however, there are several other environmental conditions (i.e. solar insolation, sea-ice thickness, sea surface nutrient concentrations) that may be related to IP_{25} biosynthesis in sea-ice diatoms. Investigation of these environmental factors' relationships to IP_{25} will lead to a better understanding of what environmental factors most influence IP_{25} production and hence what specific environmental changes are recorded by fluctuations in IP_{25} concentrations in the sediment.

APPENDIX A
SELECT BERING SEA SEDIMENT CORE INFORMATION

Core number	Water depth (m)	N latitude	W longitude	Core length (cm)	Sample location
3JPC	1132	60 07.674	179 26.508	1441	Between Navarin and Pervenets Canyons
17JPC	2209	53 55.980	178 41.930	1539	Bowers Ridge
51JPC	1467	54 33.189	168 40.015	1956	Umnak Plateau

APPENDIX B
CALCULATION PROCEDURE FOR "ICE HOURS"

Daily sunrise and sunset times at specific latitude/longitude points are available from the United States Naval Observatory (USNO) at the following website http://aa.usno.navy.mil/data/docs/RS_OneDay.php. This dataset is computed using astronomical models from the Multiyear Interactive Computer Almanac which contains astronomical data for years 1800-2050.

Procedure used to calculate "ice hours" for the year 1985

1. Bimonthly sunrise and sunset times for 1985 at each sample site were obtained from the United States Naval Observatory website. Sunlight data from the year 1985 was selected because 1985 is in the middle of the 1979-1992 sea-ice concentration data from Schweitzer (1995) utilized throughout this study. The bimonthly interval for sunlight data was used to best represent changes in daylight hours throughout the year while trying to minimize the number of data points needed to do so.

2. Hours of sunlight/day for every 1st and 16th day of the month (1st and 15th day of February) in 1985 at each sample site were calculated by subtracting the sunset time from the sunrise time. Then the number of hours of sunlight/day was multiplied by the number of days (14-16) until the next sunlight data sampling day, to represent total hours of sunlight/half month interval.

   For example, at a given site there are 5.6 hours of sunlight on January 1 and 6.4 hours of sunlight on January 16.
   (5.6 hrs on Jan 1) x (15 days until Jan 16) = 84 total hrs of sunlight/Jan 1-15
   (6.4 hrs on Jan 16) x (16 days until Feb 1) = 102.4 total hrs of sunlight/Jan 16-31

3. The number of hours of sunlight/half month interval was then multiplied by the respective mean monthly sea-ice concentration (0-100%) ((Edwards, 1989; NASA, 1992; NSIDC, 1992; 1993; Schweitzer 1995) for each site throughout the year, to represent number of "ice hours" for that bimonthly interval.

   For example, the site at which there are 84 total hours of sunlight from January 1 through January 15, has a mean monthly January sea-ice concentration of 48%.
   (84 total hrs of sunlight/Jan1-15) x (0.48 sea-ice coverage) = 40.32 "ice hours" for Jan 1-15.

4. All 24 bimonthly "ice hours" values (i.e. Jan 1-15, Jan 16-31, Feb1-14, Feb 15-28, etc.) were summed to calculate total "ice hours" for the year 1985.

APPENDIX C
TABLES OF DATA

The following are tables of data utilized in this study. Some data were not available for all samples and these are indicated by blank spaces in the tables. A Data Key is provided below to aid in the identification of abbreviated data titles.

Data Key

Table A.1 and Table A.2. Sample Identification and Site Location and Water Depth Data

"Paris ID"= Sample identification from analysis in Paris, France
"Sharko ID"= Sample identification from analysis by C. Sharko in Amherst, MA

Table A.3 and Table A.4. Sediment Analysis Data

"µg IP_{25}/g TOC" = IP_{25} concentration normalized to total organic carbon
"wt % TOC" = Weight percent of dry sediment contributed by organic carbon
"wt% TN" = Weight percent of dry sediment contributed by nitrogen
"C/N ratio" = Carbon to nitrogen ratio of dry sediment
"µg IP_{25}/g dry sed." = IP_{25} concentration per gram dry sediment

Table A.5 and Table A.6. Sea Surface Condition Data

"Avg. annual SST" = Average annual sea surface temperature
"Avg. annual SSS" = Average annual sea surface salinity
"Avg. August SST"= Average August sea surface temperature
"Avg. August SSS" = Average August sea surface salinity

Table A.1. Bering Sea Sample Identification and Site Location and Water Depth Data

Paris ID	Station Name	Sharko ID	Latitude (°N)	Longitude (°W)	Water Depth (m)
BER 001	NEC5	BER 001	61.382	171.962	60
CS_32	SEC5	BER 002	61.567	172.917	67
CS_03	SWC5	BER 004	61.884	174.358	75
CS_33	NWC5	BER 006	62.057	175.207	82
BER 007	DLN5	BER 007	62.156	176.025	95
CS_09	NWC4	BER 009	62.388	174.553	71
BER 014	SWC4	BER 014	62.244	173.742	61
CS_34	SIL4	BER 015	62.084	172.941	58
BER 016	SEC4	BER 016	61.933	172.211	57
CS_26	NEC4	BER 017	61.772	171.315	55
CS_04	SEC2.5	BER 020	63.500	171.848	48
CS_37	POP4	BER 023	62.401	172.689	58
BER 033	SWC3A	BER 033	62.755	172.7	62
CS_02	NEC1	BER 040	62.756	169.584	42
CS_07	SEC1	BER 041	62.995	170.262	38
CS_14	NOM5	BER 061	64.363	168.033	37
CS_21	NOM1	BER 065	64.472	170.845	45
CS_11	RUS2	BER 067	64.662	169.935	46
CS_15	RUS4	BER 069	64.644	168.129	35
BER 071	RUSA	BER 071	64.798	169.03	46
CS_29	KNG1	BER 073	64.954	169.89	48
CS_16	CPW1	BER 074	65.175	169.668	45
CS_28	CPW3	BER 076	65.175	168.392	47
BER 077	LDI2	BER 077	65.412	168.433	60
CS_06	SPH5	BER 094	64.205	166.802	31
CS_41	SPH4	BER 095	64.050	167.18	33
CS_40	SPH3	BER 096	63.855	167.593	35
CS_38	SPH1	BER 103	63.490	168.31	28
CS_27	NWC2.5	BER 111	63.025	173.44	72
CS_08	VNG4	BER 113	62.751	173.402	70
BER 116	SWC3	BER 116	62.577	173.065	64
CS_20	POP4	BER 117	62.407	172.691	60
CS_39	NEC1	BER 123	62.757	169.581	42
BER 137	NEC3	BER 137	62.055	170.630	49
BER 139	SEC5	BER 139	61.560	172.917	68
CS_36	NWC5	BER 143	62.055	175.197	82
BER 144	DLN5	BER 144	62.149	176.021	82
CS_35	NWC4	BER 146	62.387	174.542	73
BER 164	DBSB	BER 164	61.613	177.122	119
BER 166	DBSC	BER 166	61.236	177.792	145
BER 168	DBSD	BER 168	60.84	178.492	175
BER 170	DBSE	BER 170	60.502	179.112	438
BER 172	DBS1	BER 172	60.026	179.656	2410

Table A.2. Chukchi Sea Sample Identification and Site Location and Water Depth Data

Paris ID	Station Name	Sharko ID	Latitude (°N)	Longitude (°W)	Water Depth (m)
CS_22	BPLN-100	CHU 001	72.05	164.600	38.4
CS_19	BPLN-80	CHU 002	71.7405	164.591	36.6
CS_01	BPLN-60	CHU 003	71.3978	164.600	42
CHU 004	BPLN-40	CHU 004	71.0664	164.589	40.2
CS_12	BPLN-20	CHU 005	70.7365	164.609	45.7
CS_17	BPL-50	CHU 006	70.4053	164.587	42
CS_42	BPL-35	CHU 007	70.214	164.115	34.7
CS_25	XBW-5	CHU 008	70.751	160.266	34.7
CS_10	BW-12	CHU 010	70.808	160.381	45.7
CS_24	BCL-12	CHU 015	69.036	166.586	32.9
CS_31	BCL-50	CHU 016	69.4901	167.777	45.7
CS_23	BCLN40	CHU 017	70.1488	167.779	47.5
CS_30	BCLN80	CHU 018	70.836	167.784	54.8
CS_43	LB5	CHU 019	71.0692	166.002	42
CHU 020	LB6	CHU 020	71.4005	165.993	42
CS_13	LB6.5	CHU 021	71.599	166.005	42

Table A.3. Bering Sea Sediment Analysis Data

Sharko ID	µg IP_{25}/g TOC	wt % TOC	wt % TN	C/N ratio	µg IP_{25}/g dry sed.
BER 001	46.618	0.896	0.110	8.161	0.418
BER 002	72.285	1.294	0.127	10.189	0.935
BER 004	115.172	1.185	0.123	9.634	1.365
BER 006	84.869	1.253	0.132	9.492	1.063
BER 007	109.999	2.240	0.264	8.479	2.464
BER 009	86.317	1.931	0.237	8.144	1.667
BER 014	74.398	0.828	0.106	7.835	0.616
BER 015	146.116	0.716	0.072	9.944	1.046
BER 016	46.687	0.707	0.090	7.837	0.330
BER 017	70.385	0.812	0.087	9.287	0.572
BER 020	75.798	0.510	0.084	6.094	0.387
BER 023	110.314	0.832	0.086	9.674	0.918
BER 033	128.408	1.290	0.166	7.753	1.657
BER 040	207.029	0.272	0.058	4.732	0.564
BER 041	677.456	0.038	0.039	0.986	0.258
BER 061	174.296	0.375	0.043	8.721	0.654
BER 065	188.956	0.206	0.036	5.722	0.389
BER 067	250.770	0.726	0.103	7.063	1.821
BER 069	167.872	0.341	0.053	6.434	0.572
BER 071		0.214	0.031	6.925	0.293
BER 073	210.542	0.322	0.038	8.473	0.679
BER 074	318.216	0.246	0.062	3.980	0.783
BER 076	96.894	0.481	0.080	5.993	0.466
BER 077	161.680	0.586	0.067	8.761	0.947
BER 094	127.267	0.676	0.070	9.723	0.860
BER 095	72.554	0.431	0.082	5.239	0.313
BER 096	108.371	0.567	0.096	5.908	0.614
BER 103	137.343	0.459	0.074	6.197	0.630
BER 111	39.813	1.973	0.259	7.606	0.785
BER 113	155.962	1.689	0.222	7.616	2.634
BER 116	116.418	1.577	0.197	8.012	1.836
BER 117	96.988	0.665	0.079	8.418	0.645
BER 123	115.738	0.518	0.057	9.171	0.600
BER 137	75.894	0.982	0.120	8.172	0.745
BER 139	57.073	1.375	0.175	7.863	0.785
BER 143	135.407	1.426	0.142	10.042	1.931
BER 144	161.607	2.246	0.270	8.311	3.629
BER 146	139.393	1.191	0.162	7.352	1.660
BER 164	112.486	1.554	0.199	7.811	1.748
BER 166	75.517	1.266	0.158	8.002	0.956
BER 168	154.847	0.829	0.098	8.419	1.284
BER 170		0.189	0.033	5.757	0.385
BER 172	105.045	1.485	0.166	8.933	1.560

Table A.4. Chukchi Sea Sediment Analysis Data

Sharko ID	μg IP_{25}/g TOC	wt % TOC	wt % TN	C/N ratio	μg IP_{25}/g dry sed.
CHU 001	2009.821	0.913	0.115	7.968	18.341
CHU 002	1702.703	0.651	0.086	7.571	11.090
CHU 003	1463.957	1.237	0.145	8.521	18.105
CHU 004	1227.029	1.005	0.120	8.391	12.337
CHU 005	989.143	1.363	0.155	8.818	13.481
CHU 006	716.993	0.971	0.107	9.077	6.964
CHU 007	753.379	0.269	0.041	6.631	2.030
CHU 008	425.618	0.403	0.042	9.497	1.715
CHU 010	820.527	0.783	0.087	8.985	6.426
CHU 015	461.696	1.584	0.134	11.811	7.315
CHU 016	420.635	1.278	0.138	9.260	5.377
CHU 017	413.423	1.207	0.130	9.255	4.990
CHU 018	536.441	1.366	0.167	8.170	7.326
CHU 019	985.493	1.259	0.138	9.114	12.411
CHU 020	1489.965	1.358	0.160	8.491	20.231
CHU 021	1167.713	1.295	0.153	8.477	15.123

Table A.5. Bering Sea Surface Condition Data

Sharko ID	Months of sea ice per year	Avg. annual SST (°C)	Avg. annual SSS (psu)	Avg. August SST (°C)	Avg. August SSS (psu)
BER 001	4.5	5.11	31.48	8.41	31.42
BER 002	4.5	5.25	31.58	8.51	31.52
BER 004	4.5	5.34	31.84	8.67	31.78
BER 006	4.5	5.71	31.86	8.51	31.70
BER 007	4.5	5.82	31.93	8.61	31.74
BER 009	5	5.61	31.74	8.44	31.61
BER 014	5	5.6	31.56	8.44	31.45
BER 015	5	5.52	31.42	8.40	31.31
BER 016	5	5.17	31.58	8.51	31.52
BER 017	5	5.11	31.48	8.41	31.42
BER 020	5				
BER 023	5	5.52	31.42	8.40	31.31
BER 033	5	5.52	31.42	8.40	31.31
BER 040	5.5	5.43	31.2	8.29	31.08
BER 041	9	5.42	31.34	8.21	31.23
BER 061	6	5.34	31.51	7.72	31.14
BER 065	5.5	5.27	31.85	7.48	31.55
BER 067	6	5.29	31.7	7.56	31.38
BER 069	6	5.34	31.51	7.72	31.14
BER 071	6	5.29	31.7	7.56	31.38
BER 073	6	5.29	31.7	7.56	31.38
BER 074	6	7.1	32.05	8.23	30.74
BER 076	7	7.2	32.12	8.51	31.04
BER 077	9	7.2	32.12	8.51	31.04
BER 094	9				
BER 095	6.5	5.42	31.27	7.93	30.84
BER 096	5.5	6.11	30.39	8.97	30.06
BER 103	6				
BER 111	5	6.1	31.41	8.35	31.23
BER 113	5	5.6	31.56	8.44	31.45
BER 116	5	5.6	31.56	8.44	31.45
BER 117	5	5.52	31.42	8.40	31.31
BER 123	5.5	5.43	31.2	8.29	31.08
BER 137	5	5.42	31.34	8.21	31.23
BER 139	4.5	5.17	31.58	8.51	31.52
BER 143	4.5	5.71	31.86	8.51	31.70
BER 144	4.5	5.82	31.93	8.61	31.74
BER 146	5	5.61	31.74	8.44	31.61
BER 164	4	5.66	32.14	8.99	32.01
BER 166	3	5.66	32.14	8.99	32.01
BER 168	3	5.76	32.43	9.31	32.32
BER 170	1.5	5.85	32.48	9.40	32.35
BER 172	0.5	5.85	32.48	9.40	32.35

Table A.6. Chukchi Sea Surface Condition Data

Sharko ID	Months of sea ice per year	Avg. annual SST (°C)	Avg. annual SSS (psu)	Avg. August SST (°C)	Avg. August SSS (psu)
CHU 001	11	1.47	29.93	2.18	27.24
CHU 002	11	2.32	30.33	3.39	27.54
CHU 003	11	2.32	30.33	3.39	27.54
CHU 004	11	2.32	30.33	3.39	27.54
CHU 005	9	3.28	30.75	4.75	28.05
CHU 006	8.5	3.28	30.75	4.75	28.05
CHU 007	8.5	3.28	30.75	4.75	28.05
CHU 008					
CHU 010	11				
CHU 015	10	4.3	31.32	6.01	28.84
CHU 016	8	3.79	31.32	5.49	28.79
CHU 017	8	3.14	30.86	4.47	27.99
CHU 018	9	3.14	30.86	4.47	27.99
CHU 019	9	2.33	30.4	3.41	27.48
CHU 020	10.5	2.33	30.38	3.43	27.55
CHU 021	10.5	2.33	30.4	3.41	27.48

APPENDIX D
SUPPLEMENTAL GRAPHS OF DATA

Elemental Analysis Graphical Data

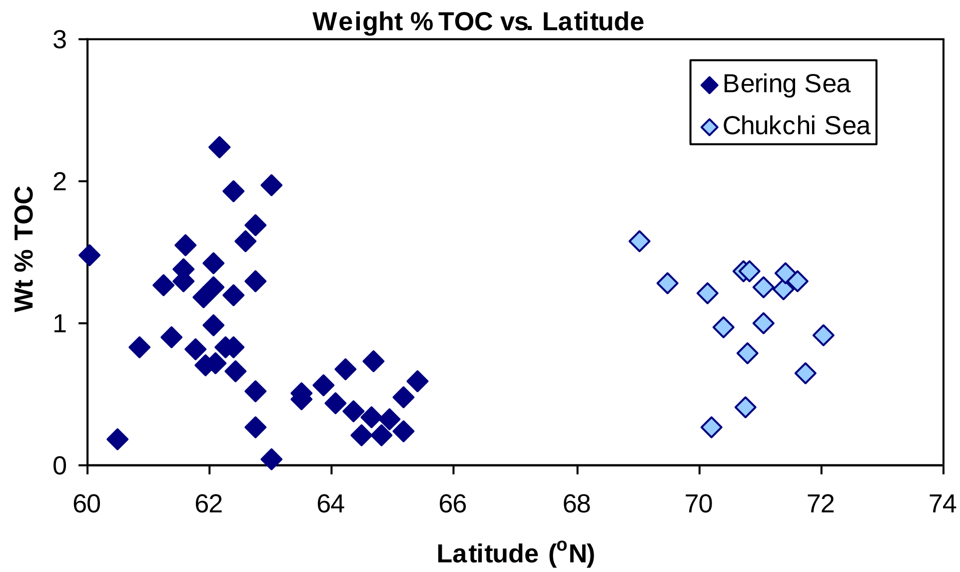

Figure A.1. Weight % total organic carbon (TOC) for Bering and Chukchi Sea sediments

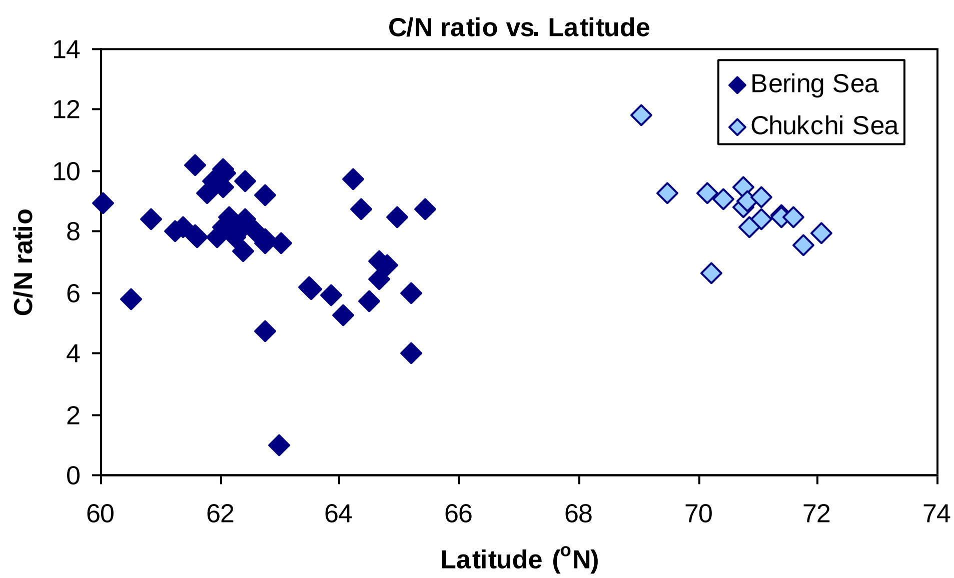

Figure A.2. Carbon/Nitrogen ratios for Bering and Chukchi Sea sediments

Sea Surface Condition Graphical Data

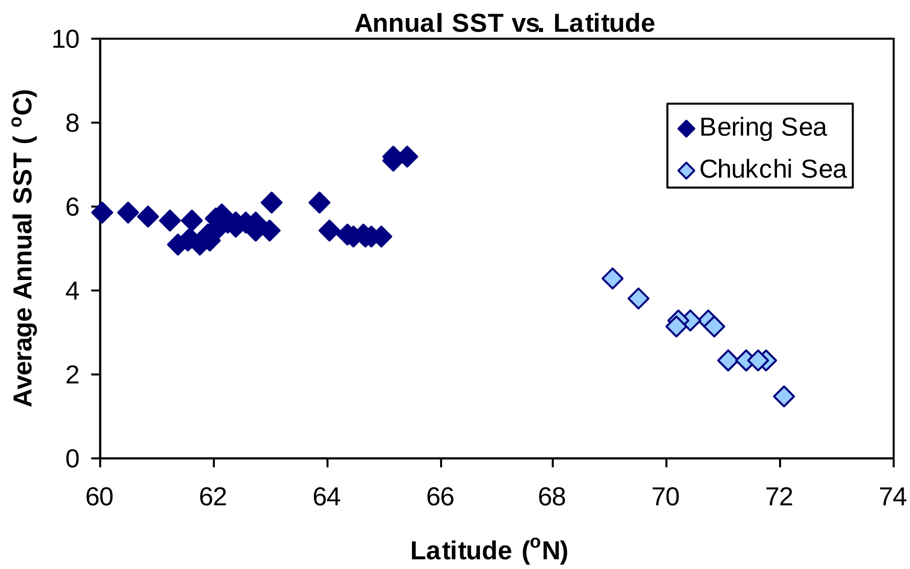

Figure A.3. Average annual sea surface temperatures of Bering and Chukchi Sea sample sites plotted against latitude
SST data from (Levitus and Gelfeld 1992, Levitus et al. 1994)

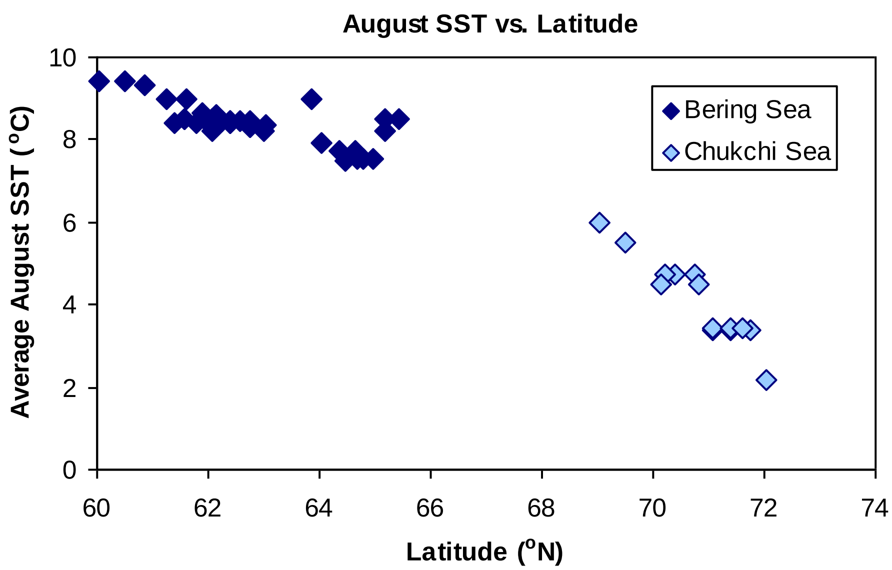

Figure A.4. Average August sea surface temperatures of Bering and Chukchi Sea sample sites plotted against latitude
SST data from (Levitus and Gelfeld 1992, Levitus et al. 1994)

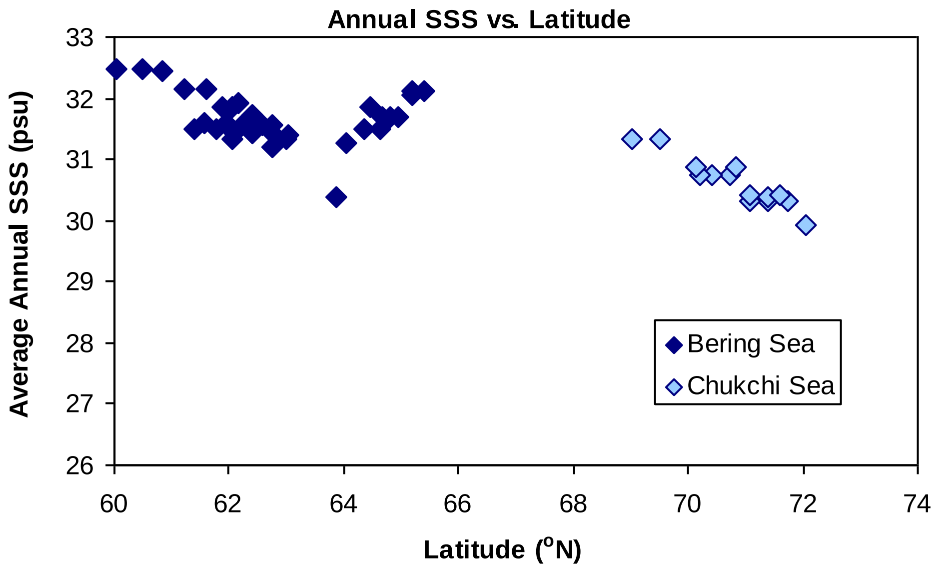

Figure A.5. Average annual sea surface salinities of Bering and Chukchi Sea sample sites plotted against latitude
SSS data from (Levitus and Gelfeld 1992, Levitus et al. 1994)

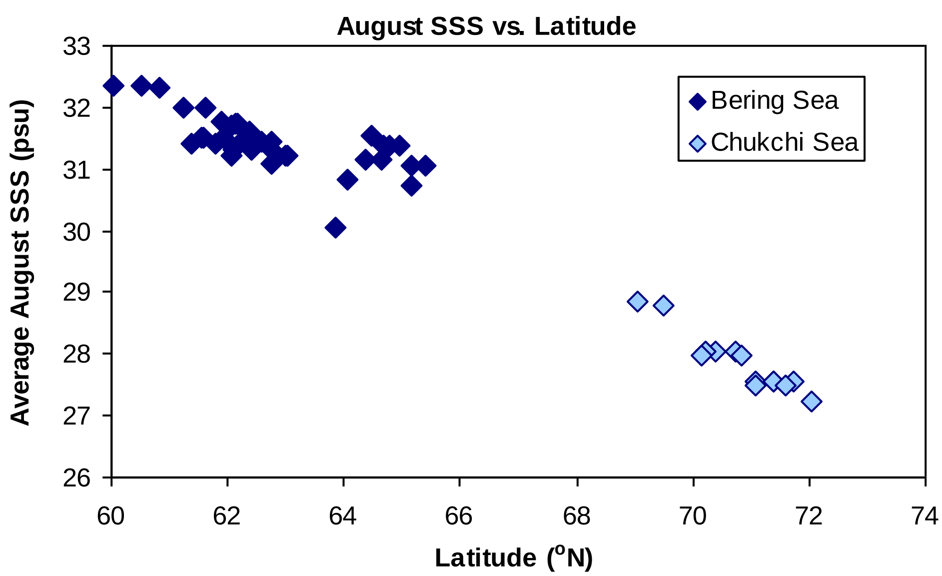

Figure A.6. Average August sea surface salinities of Bering and Chukchi Sea sample sites plotted against latitude
SSS data from (Levitus and Gelfeld 1992, Levitus et al. 1994)

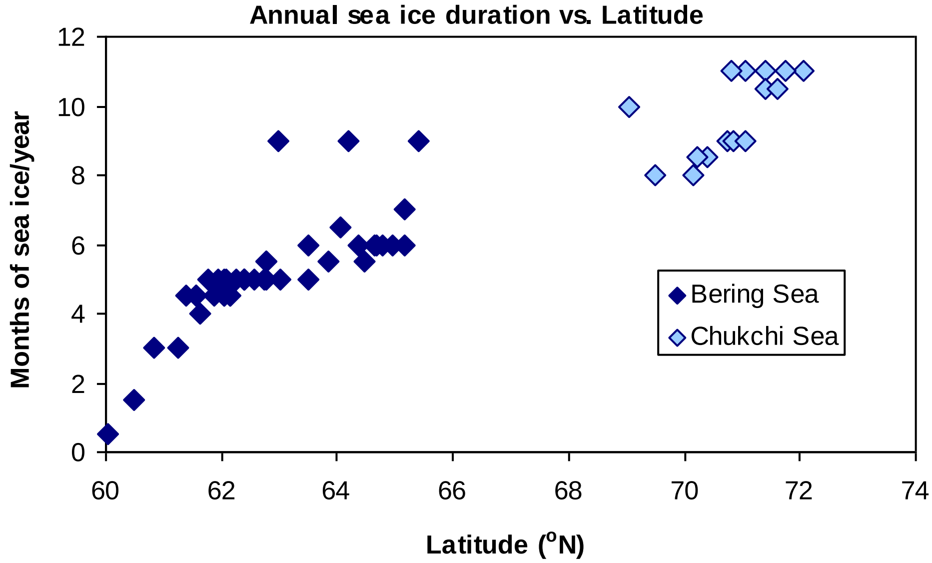

Figure A.7. Mean annual sea-ice duration of Bering and Chukchi Sea sample sites plotted against latitude
Sea-ice data from (Edwards 1989; NASA 1992; NSIDC 1992; 1993; Schweitzer 1995)

APPENDIX E
SELECTED GAS CHROMATOGRAPH/MASS SPECTROMETRY DATA

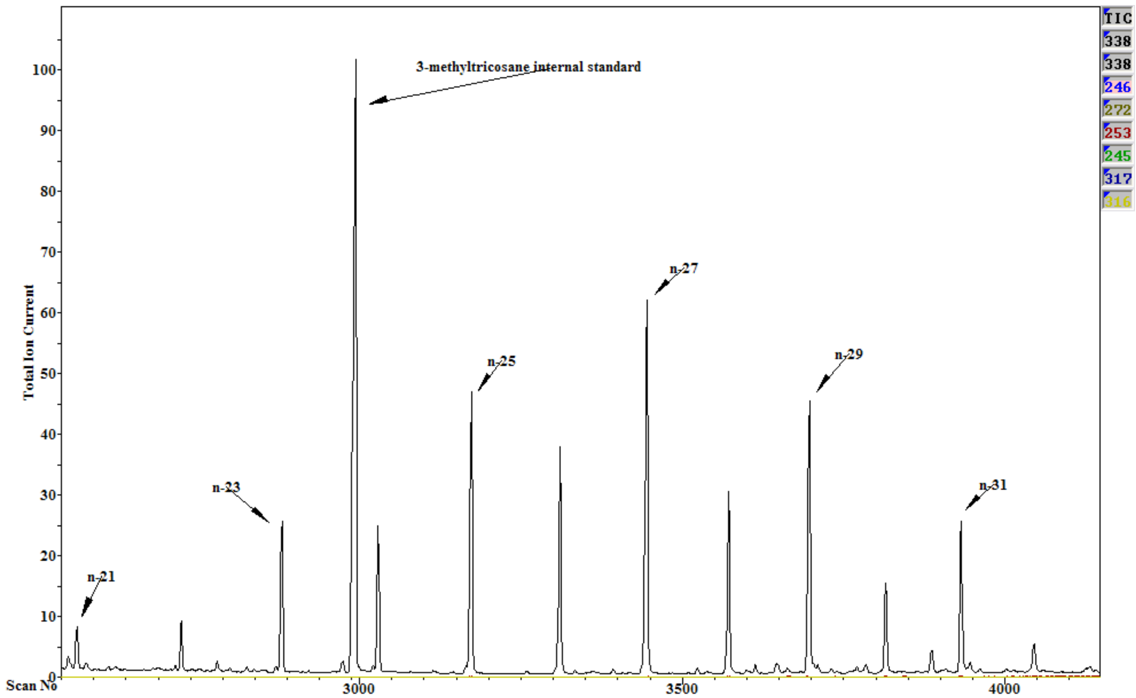

Figure A.8. Gas chromatogram (Scan mode) for sample “BER 009, first fraction eluted from silica gel column with hexane;” several alkanes are identified

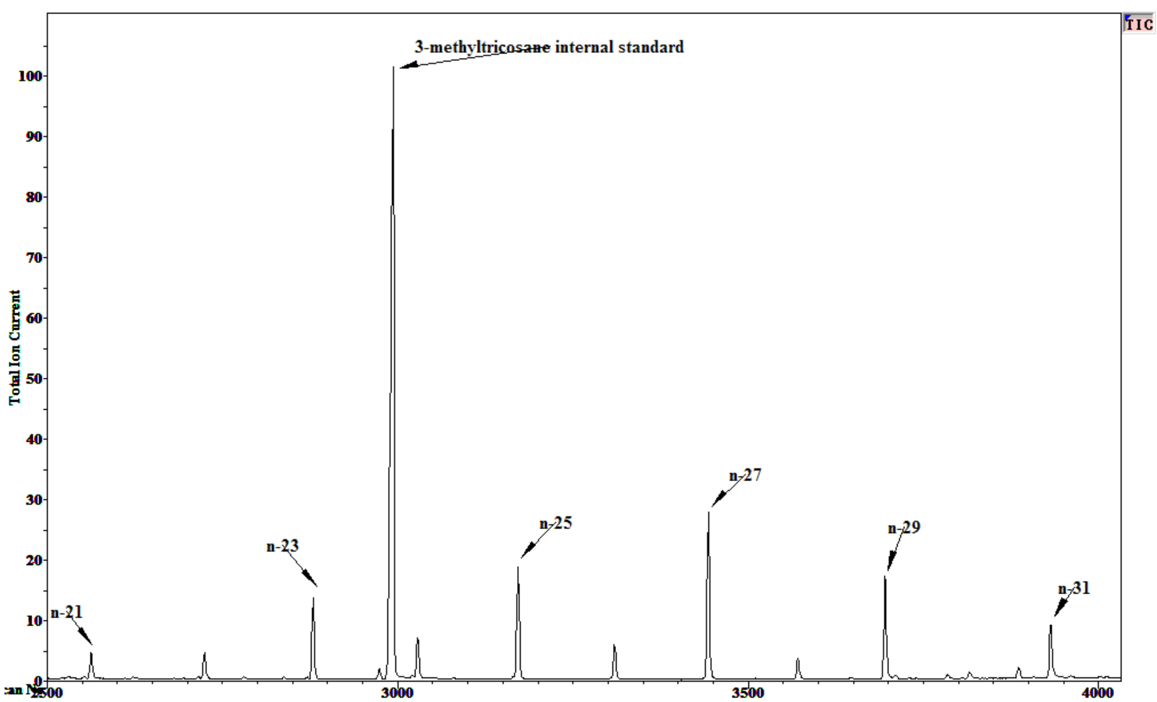

Figure A.9. Gas chromatogram (Scan mode) for sample “BER 139, first fraction eluted from silica gel column with hexane;” several alkanes are identified

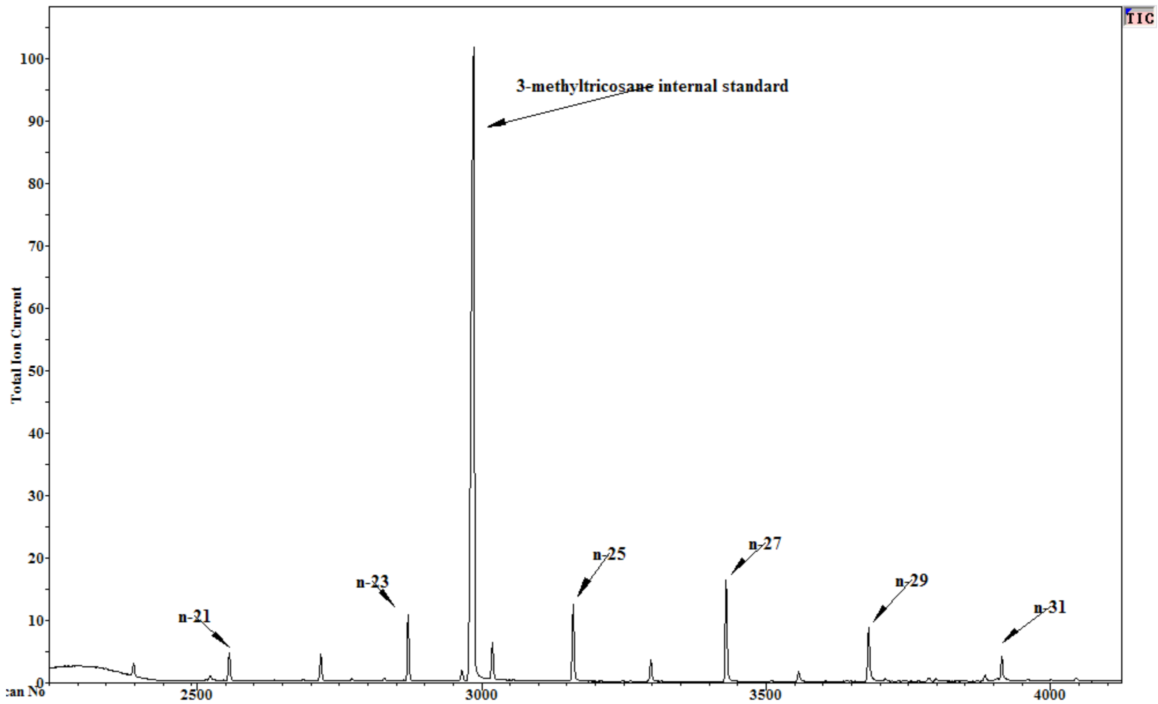

Figure A.10. Gas chromatogram (Scan mode) for sample "CHU 005, first fraction eluted from silica gel column with hexane;" several alkanes are identified

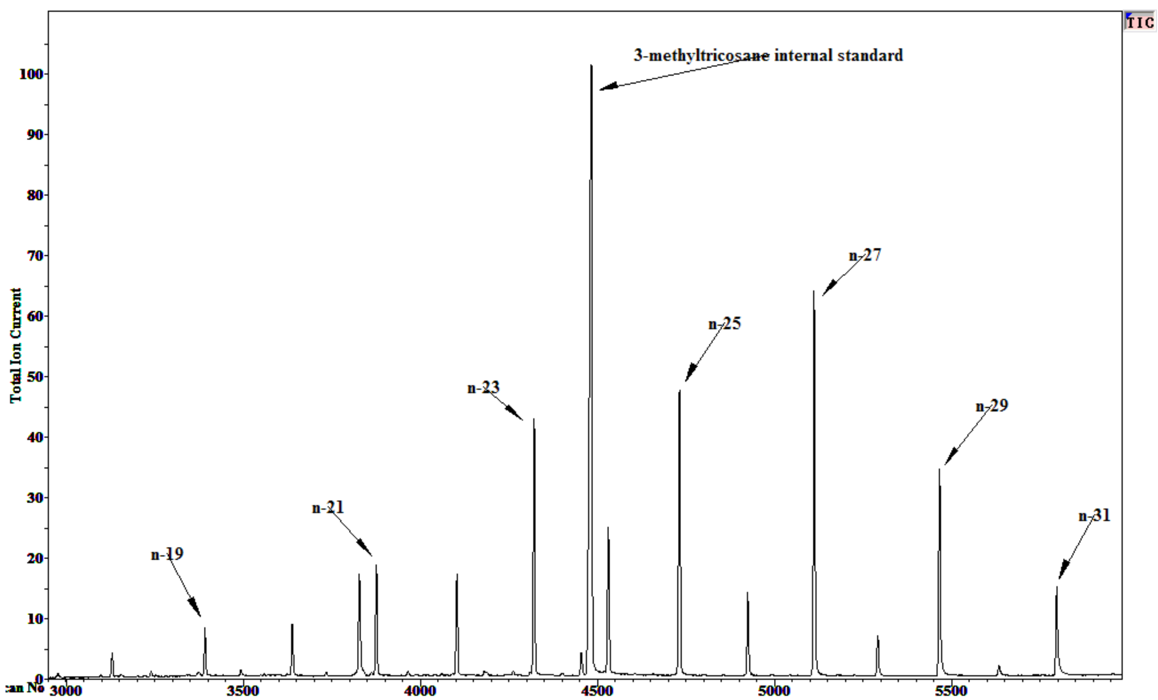

Figure A.11. Gas chromatogram (Selected Ion Monitoring (SIM) mode; monitored ions: 140, 266, 338, 350) for sample "CHU 005, first fraction eluted from silica gel column with hexane;" several alkanes are identified

BIBLIOGRAPHY

Alexander, V. and H.J. Niebauer, 1981. Oceanography of the eastern Bering Sea-ice-edge zone in spring. *Limnology and Oceanography* 26, 1111-1125.

Andrews, J.T., Belt, S.T., Olafsdottir, S., Massé, G., Vare, L.L., 2009. Sea ice and marine climate variability for NW Iceland/Denmark Strait over the last 2000 cal. yr BP. *Holocene* 19, 775-784.

Armand, L.K., Crosta, X., Romero, O., and Pinchon, J.J. 2005. The biogeography of major diatom taxa in Southern Ocean sediments: 1. Sea-ice related species. *Palaeogeography, Palaeoclimatology, Palaeoecology* 223, 96-126.

Arrigo, K.R., 2003. Primary Production in Sea-ice. In: *Sea-ice: An Introduction to its Physics Chemistry Biology and Geology*, first ed, (Eds. D.N. Thomas and G.S. Dieckmann), p143-183, Blackwell, Oxford.

Barron, J.A., 1993. Diatoms. In: J.H. Lipps (Ed.), *Fossil prokariotes and protists*, Blackwell Scientific Publications, Oxford, 155-167.

Belt, S.T., Allard, W.G., Masse, G., Robert, J.M., Rowland, S.J., 2000. Highly branched isoprenoids (HBIs): Identification of the most common and abundant sedimentary isomers. *Geochimica et Cosmochimica Acta* 64, 3839-3851.

Belt, S.T., Masse, G., Allard, W.G., Robert, J.M., Rowland, S.J., 2001. C_{25} highly branched isoprenoid alkenes in planktonic diatoms of the *Pleurosigma* genus. *Organic Geochemistry* 32, 1271-1275.

Belt, S.T., Massé, G., Rowland, S.J., Poulin, M., Michel, C., LeBlanc, B., 2007. A novel chemical fossil of palaeo sea-ice: IP_{25}. *Organic Chemistry* 38, 16-27.

Belt, S.T., Massé, G., Vare, L.L., Rowland, S.J., Poulin, M., Sicre, M.-A., Sampei, M., Fortier, L., 2008. Distinctive 13C isotopic signature distinguishes a novel sea-ice biomarker in Arctic sediments and sediment traps. *Marine Chemistry* 112, 158-167.

Brassel, S.C., Eglinton, G., Marlowe, I.T., Pflaumann, U., Sarnthein, M., 1986. Molecular stratigraphy: a new tool for climatic assessment. *Nature* 320, 129-133.

Broecker, W.S., 1997. Thermohaline circulation, the Achilles heel of our climate system: will man-made CO2 upset the current balance? *Science* 278, 1582–1588.

Budikova, D., 2009. Role of Arctic sea-ice in global atmospheric circulation: A review. *Global and Planetary Change* 68, 149-163.

Caissie, B., Brigham-Grette, J., Lawrence, K.T., Herbert, T.D., Cook, M.S., (in press). Last Glacial Maximum to Holocene Sea Surface Conditions at Umnak Plateau, Bering Sea as Inferred from Diatom, Alkenone, and Stable Isotope Records. *Paleoceanography* 25, PA1206, doi:10.1029/2008PA001671.

Conte, M.H., Sicre, M.A., Rühlemann, C., Weber, J.C., Schulte, S., Schulz-Bull, D., Blanz, T., 2006. Global temperature calibration of the alkenone unsaturation index ($U^{K'}_{37}$) in surface waters and comparison with surface sediments. *Geochemistry Geophysics Geosystems* 7, 1-22.

de Vernal, A. and Hillaire-Marcel, C., 2000. Sea-ice cover, sea-surafce salinity and halo-/thermocline structure of the northwest North Atlantic: modern versus full glacial conditions. *Quaternary Science Reviews* 19, 65-85.

de Vernal, A., Eynaud, F., Henry, M., Hillaire-Marcel, C., Londeix, L., Mangin, S., Matthiessen, Marret, F., Radi, T., Rochon, A., Solignac, S., Turon, J.-L., 2005. Reconstruction of sea-surface conditions at middle to high latitudes of the Northern Hemisphere during the Last Glacial Maximum (LGM) based on dinoflagellate cyst assemblages. *Quaternary Science Reviews* 24, 897-924.

Dieckmann, G.S. and Hellmer, H.H., 2003. The Importance of Sea-ice: An Overview. In: *Sea-ice: An Introduction to its Physics Chemistry Biology and Geology*, first ed, (Eds. D.N. Thomas and G.S. Dieckmann), p1-21, Blackwell, Oxford.

Dunlop, R.W. and Jefferies, P.R., 1985. Hydrocarbons of the hypersaline basins of Shark Bay, Western Australia. *Organic Geochemistry* 8, 313-320.

Edwards, Margaret H., 1989. Global gridded elevation and bathymetry (ETOPO5): Digital raster data on a 5-minute geographic (lat/long) 2160x4320 (centroid-registered) grid: U.S. National Oceanic and Atmospheric Administration, National Geophysical Data Center, Boulder, Colorado.

Expedition 323 Scientists, 2010. Bering Sea paleoceanography: Pliocene–Pleistocene paleoceanography and climate history of the Bering Sea. *IODP Prel. Rept.*, 323. doi:10.2204/iodp.pr.323.2010.

Gearing, P., Gearing, J.N., Lytle, T.F., Lytle, J.S., 1976. Hydrocarbons in 60 Northeast Gulf of Mexico sediments: a preliminary survey. *Geochimica et Cosmochimica Acta* 40, 1005-1017.

Gosselin, M., Levasseur, M., Wheeler, P.A., Horner, R.A., Booth, B.C., 1997. New measurements of phytoplankton and ice algal production in the Arctic Ocean. *Deep-Sea Research II* 44, 1623-1644.

Gradinger, R. and Ikävalko, J., 1998. Organism incorporation into newly forming Arctic sea-ice in the Greenland Sea. *Journal of Plankton Research* 20, 871-886.

Gradinger, R., Friedrich, C., Spindler M., 1999. Abundance, biomass, and composition of the sea ice biota of the Greenland Sea pack ice. *Deep-Sea Research II* 46, 1457-1472.

Gradinger, R., 2009. Sea-ice algae: Major contributors to primary production and algal biomass in the Chukchi and Beaufort Seas during May/June 2002. *Deep Sea Research II* 56, 1201-1212.

Grebmeier, J.M., Overland, J.E., Moore, S.E., Farley, E.V., Carmack, E.C., Cooper, L.W., Frey, K.E., Helle, J.H., McLaughlin, F.A., McNutt, S.L., 2006. A Major Ecosystem Shift in the Northern Bering Sea. *Science* 311, 1461-1464.

Harada, N., Shin, K.H., Murata, A., Uchida, M., Nakatani, T., 2003. Characteristics of alkenones synthesized by a bloom of Emiliania huxleyi in the Bering Sea. *Geochimica et Cosmochimica Acta* 67, 1507-1519.

Hassol, S., 2004. Impacts of a Warming Arctic: Arctic Climate Impact Assessment. Cambridge University Press, Cambridge, UK.

Herbert, T.D., and Schuffert, J.D., 1998. Alkenone Unsaturation of Late Miocene Through Late Pliocene Sea-Surface Temperatures at Site 958. In: *Proceedings of Ocean Drilling Program Science Results* (Ed. J.V. Firth) 17-21.

Hird, S.J., Evens, R., Rowland, S.J., 1992. Isolation and characterization of sedimentary and synthetic highly branched C20 and C25 monoenes. *Marine Chemistry* 37, 117-129.

Horner, R. and Schrader, G.C., 1982. Relative Contributions of Ice Algae, Phytoplankton, and Benthic Microalgae to Primary Production in Nearshore Regions of the Beaufort Sea. *Arctic* 35, 485-503.

Horner, R.A., 1985. Ecology of sea-ice microalgae, In: *Sea-ice Biota*, (Ed. R.A. Horner), p83-103, CRC Press, Boca Raton, Florida.

Internet Reference 1: http://aa.usno.navy.mil/data/docs/RS_OneDay.php

http://disc.gsfc.nasa.gov/oceancolor/scifocus/oceanColor/bering_sea.shtml

Johannessen, O.M., Shalina, E.V., Miles, M.W., 1999. Satellite Evidence for an Arctic Sea-ice Cover in Transformation. *Science* 286, 1937-1939.

Johns, L., Wraige, E.J., Belt, S.T., Lewis, C.A., Massé, G., Robert, J.M., Rowland, S.J., 1999. *Organic Geochemistry* 30, 1471-1475.

Kim, J.-H., Schouten, S., Hopmans, E.C., Donner, B., Sinning-Damste, J.S., 2008. Global sediment core-top calibration of the TEX_{86} paleothermometer in the ocean. *Geochimica et Cosmochimica Acta* 72, 1154-1173.

Kunz-Pirrung, M., Gersonde, R., Hodell, D.A., 2002. Mid-Brunhes century-scale diatom sea surface temperature and sea-ice records from the Atlantic sector of the Southern Ocean (ODP Leg 177, sites 1093, 1094 and core PS2089-2). *Palaeogeography, Palaeoclimatology, Palaeoecology* 182, 305-328.

Lalande, C., Grebmeier, J.M., Wassmann, P., Cooper, L.W., Flint, M.V., Sergeeva, V.M., 2007. Export fluxes of biogenic matter in the presence and absence of seasonal sea-ice cover in the Chukchi Sea. *Continental Shelf Research* 27, 2051-2065.

Laskar, J., Robutel, P., Joutel, F., Gastineau, M., Correia, A.C.M., Levrard, B., 2004. A long term numerical solution for the insolation quantities of the Earth. *Astronomy and Astrophysics* 428, 261-285, DOI: 10.1051/0004-6361:20041335. <http://www.imcce.fr/Equipes/ASD/insola/earth/earth.html>

Lee, S.H., Whitledge, T.E., Kang, S., 2008. Springtime production of ice algae in the landfast sea-ice zone at Barrow, Alaska. *Journal of Experimental Marine Biology and Ecology* 367, 204-212.

Leventer, A., 2003. Particulate Flux from Sea-ice in Polar Waters, In: *Sea-ice: An Introduction to its Physics Chemistry Biology and Geology*, first ed, (Eds. D.N. Thomas and G.S. Dieckmann), p303-332, Blackwell, Oxford.

Levitus, S. and Gelfeld, R., 1992. NODC Inventory of Physical Oceanographic Profiles. Key to Oceanographic Records Documentation No. 18, NODC, Washington D.C.

Levitus, S., Gelfeld, R., Boyer, T., Johnson, D., 1994. Results of the NODC and IOC Oceanographic Data Archaeology and Rescue Projects. Key to Oceanographic Records Documentation, No. 19, NODC, Washington D.C.

Lizotte, M.P., 2003. The Microbiology of Sea-ice, In: *Sea-ice: An Introduction to its Physics Chemistry Biology and Geology*, first ed, (Eds. D.N. Thomas and G.S. Dieckmann), p184-210, Blackwell, Oxford.

Massé, G., Rowland, S.J., Sicre, M.A., Jacob, J., Jansen, E., Belt, S.T., 2008. Abrupt climate changes for Iceland during the last millennium: Evidence from high resolution sea-ice reconstructions. *Earth and Planetary Research letters* 269, 565-569.

McBean, G., Alekseev, G., Chen, D., Førland, E., Fyfe, J., Groisman, P.Y., King, R., Melling, H.,Vose, R., Whitfield, P.H., 2005. Arctic climate: past and present. Arctic climate impact assessment. Scientific Report. Cambridge University Press.

McConville, M.J., 1985. Chemical composition and biochemistry of microalgae, In: *Sea-ice Biota*, (Ed. R.A. Horner), p105-157. CRC Press, Boca Raton, Florida.

Meguro, H., Ito, K., Fukushim, H., 1967. Ice flora (bottom type): a mechanism of primary production in polar seas and growth of diatoms in sea-ice. *Arctic* 20, 114-133.

Meier, W., Stroeve, J., Fetterer, F., Knowles, K., 2005. Reductions in Arctic Sea-ice Cover No Longer Limited to Summer. *Eos* 86, 326-327.

Menzel, D., Hopmans, E.C., Schouten, S., Sinninghe Damsté, J.S., 2006. Membrane tetraether lipids of planktonic Crenarchaeota in Pliocene sapropels of the eastern Meditteranean Sea. *Paleogeography, Palaeoclimatology, Palaeoecology* 239, 1-15.

Meyers, P. A., 1994. Preservation of elemental and isotopic source identification of sedimentary organic matter. *Chem. Geol.* 114, 289–302

Michel, C., Legendre, L., Ingram, R.G., Gosselin, M., Levasseur, M., 1996. Carbon budget of sea-ice algae in spring: evidence of a significant transfer to zooplankton grazers. *Journal of Geophysical Research* 101, 18345-18360.

Muller, P.J., Kirst, G., Ruhland, G., von Storch, I., Rosell-Melé, A., 1998. Calibration of the alkenone paleotemperature index $U^{K'}_{37}$ based on core-tops from the eastern South Atlantic and the global ocean (60^oN-60^oS). *Geochimica et Cosmochimica Acta* 62, 1757-1772.

Müller, J., Massé, G., Stein, R., Belt, S.T., 2009.Variability of sea-ice conditions in the Fram Strait over the past 30,000 years. *Nature Geoscience* 2, 772-776.

NASA, 1992. Radiances on a North Polar Stereographic Grid 4/1/ 87 - 8/20/87 and Arctic and Antarctic Sea-ice Concentrations 10/25/78 - 8/20/87 volume 7 of Nimbus-7 Scanning Multichannel Microwave Radiometer (SMMR) Polar Data: Goddard Space Flight Center SMMR Polar Data volume 7.

Nichols, P.D., Volkman, J.K., Palmisano, A.C., Smith, G.A., White, D.C., 1988. Occurrence of an isoprenoid C-25 diunsaturated alkene and high neutral lipid-content in Antarctic sea-ice diatom communities. *Journal of Phycology* 24, 90-96.

Niebauer, H.J., Alexander, V., Henrichs, S., 1990. Physical and Biological Oceanographic Interaction in the Spring Bloom at the Bering Sea Marginal Ice Edge Zone. *Journal of Geophysical Research* 95, 22229-22241.

Niebauer, H.J., Alexander, V., Henrichs, S., 1995. A time-series study of the spring bloom at the Bering Sea-ice edge I. Physical processes, chlorophyll and nutrient chemistry. *Continental Shelf Research* 15, 1859-1877.

NSIDC, 1992. DMSP SSM/I ice concentration grids for the polar regions: DMSP SSM/I brightness temperature and sea-ice concentration grids for the polar regions on CD-ROM volume 1, revision 2.

NSIDC, 1993. DMSP SSM/I ice concentration grids for the polar regions: DMSP SSM/I brightness temperature and sea-ice concentration grids for the polar regions on CD-ROM volume 2, revision 2.

Palmisano, A.C., Lizotte, M.P., Smith, G.A., Nichols, P.D., White, D.C., Sullivan, C.W., 1988. Changes in photosynthetic carbon assimilation in Antarctic sea-ice diatoms during spring bloom: variation in synthesis of lipid classes. *Journal of Experimental Marine Biology and Ecology* 116, 1-13.

Parkinson, C.L., Rind, D., Healy, R.J., Martinson, D.G., 2001. The impact of sea-ice concentration accuracies on climate model simulations with the GISS GCM. *Journal of Climate* 14, 2606–2623.

Prahl, F.G. and Wakeham, S.G., 1987. Calibration of unsaturation patterns in long-chain ketone Compositions for palaeotemperature assessment. *Nature* 330, 367-369.

Prahl, F.G., Muehlhausen, L.A., Zahnle, D.L., 1988. Further evaluation of long-chain alkenones as indicators of paleoceanographic conditions. *Geochimica et Cosmochimica Acta* 52, 2303-2310.

Prahl, F.G., Wolfe, G.V., Sparrow, M.A., 2003. Physiological impacts on alkenone paleothermometry. *Paleoceanography* 18, 3-1 – 3-7.

Prahl, F.G., Mix, A.C., Sparrow, M.A., 2006. Alkenone paleothermometry: Biological lessons from records off western South America. *Geochimica et Cosmochimica Acta* 70, 101-117.

Rho, T., and Whitledge, T.E., 2007. Characteristics of seasonal and spatial variations of primary production over the southeastern Bering Sea shelf. *Continental Shelf Research* 27, 2556-2569.

Riebesell, U., Schloss, I., Smetakek, V., 1991. Aggregation of algae released from melting sea-ice:implications for seeding and sedimentation. *Polar Biology* 11, 239-248.

Riedel, A., Michel, C., Gosselin, M., 2006. Seasonal study of sea-ice exopolymeric substances (EPS) on the Mackenzie Shelf implications for the transport of sea-ice bacteria and algae. *Aquatic Microbial Ecology* 45, 195-206.

Riedel, A,. Michel, C., Gosselin, M., LeBlanc, B., 2008. Winter-spring dynamics in sea-ice carbon cycling in the coastal Artic Ocean. *Journal of Marine Systems* 74, 918-932.

Rochet, M., Legendre, L., Demers, S., 1986. Photosynthetic and pigment responses of sea-ice microalgae to changes in light intensity and quality. *Journal of Experimental Marine Biology and Ecology* 101, 211-226.

Rosell-Melé, A., 1998. Interhemispheric appraisal of the value of alkenone indices as temperature and salinity proxies in high-latitude locations. *Paleoceanography* 13, 694-703.

Rowland, S.J., and Robson, J.N., 1990. The Widespread Occurrence of Highly Branched Acyclic C_{20}, C_{25} and C_{30} Hydrocarbons in Recent Sediments and Biota-A Review. *Marine Environmental Research* 30, 191-216.

Rowland, S.J., Belt, S.T., Wraige, E.J., Massé, G., Roussakis, C., Robert, J.-M., 2001a. Effects of temperature on polyunsaturation in cytostatic lipids of *Haslea ostrearia*. *Phytochemistry* 56, 597-602.

Rowland, S.J., Allard, W.G., Belt, S.T., Massé, G., Robert, J.-M., Blackburn, S., Frampton, D., Revill, A.T., Volkman, J.K., 2001b. Factors influencing the distributions of polyunsaturated terpenoids in the diatom, *Rhizosolenia setigera*. *Phytochemistry* 58, 717-728.

Royer, J.F., Planton, S., Déqué, M.,1990. A sensitivity experiment for the removal of Arctic sea-ice with the French spectral general circulation model. *Climate Dynamics* 5, 1–17.

Sakamoto, T., Ikehara, M., Aoki, K., Iijima, K., Nakatsuka, T., and Wakatsuchi, M., 2005. Ice-rafted debris (IRD)-based sea-ice expansion events during the past 100 kyrs in the Okhotsk Sea: *Deep-Sea Research II* 52, 2275-2301.

Schouten, S., Hopmans, E.C., Pancost, R.D., Sinninghe Damsté, J.S., 2000. Widespread occurrence of structurally diverse tetraether membrane lipids: Evidence for the ubiquitous presence of low-temperature relatives of hyperthermophiles. *Proceedings of the National Academy of Sciences* 97, 14421-14426.

Schouten, S., Hopmans, E.C., Schefuβ, E., Sinninghe Damsté, J.S., 2002. Distributional variations in marine crenarchaeotal membrane lipids: a new tool for reconstructing ancient sea water temperatures? *Earth and Planetary Research Letters* 204, 265-274.

Schouten, S., Huguet, C., Hopmans, E.C., Kienhuis, V.M., Sinninghe Damsté, J.S., 2007. Analytical Methodology for TEX86: Paleothermometry by High-Performance Liquid Chromatography/Atmospheric Pressure Chemical Ionization-Mass Spectrometry. *Analytical Chemistry* 79, 2940-2944.

Schweitzer, Peter N., 1995. Monthly average polar sea-ice concentration: U.S. Geological Survey Digital Data Series DDS-27, U.S. Geological Survey, Reston, Virginia.

Sinninghe Damsté, J.S., Schouten, S., Hopmans, E.C., van Duin, A.C.T., Geenevasen, J.A.J., 2002. Crenarchaeol: the characteristic core glycerol dibiphytanyl glycerol tertraether membrane lipid of cosmopolitan pelagic crenarchaeota. *Journal of Lipid Research* 43, 1641-1651.

Smith, R.E.H., Clement, P., Cota, G.F., Li, W.K.W., 1987. Intracellular photosynthate allocation and the control of Arctic marine ice-algal production. *Journal of Phycology* 23, 124-132.

Smith, R.E.H., Clement, P., Head, E., 1989. Biosynthesis and photosynthate allocation patterns of high arctic ice algae. *Limnology and Oceanography* 34, 591-605.

Smith, R.E.H., Gossein, M., Taguchi, S., 1997. The influence of major inorganic nutrients on the growth and physiology of high arctic ice algae. *Journal of Marine Systems II*, 63-70.

Stabeno, P.J., Bond, N.A., Kachel, N.B., Salo, S.A., Schumacher, J.D., 2001. On the temporal variability of the physical environment over the south-eastern Bering Sea. *Fisheries Oceanography*, 10, 81-98.

Takahashi, K., 1998. The Bering and Okhotsk Seas: modern and past paleoceanographic changes and gateway impact. *Journal of Asian Earth Sciences* 16, 49-58.

Thomas, D.N. and Dieckmann, G.S., (Eds.), 2003. *Sea-ice: An Introduction to its Physics Chemistry Biology and Geology*, first ed. Blackwell, Oxford.

Vare, L.L., Massé, G., Gregory, T.R., Smart, C.W., Belt, S.T., 2009. Sea-ice variations in the Central Canadian Arctic Archipelago during the Holocene. *Quaternary Science Reviews* 28, 1354-1366.

Vinnikov, Y.V., Robock, A., Stouffer, R.J., Walsh, J.E., Parkinson, C.L., Cavalieri, D.J., Mitchell, J.F.B., Garrett, D., Zakharov, V.F., 1999. Global Warming and Northern Hemisphere Sea-ice Extent. *Science* 286, 1934-1937.

Volkman, J.K., Barrett, S.M., Dunstan, G.A., 1994. C25 and C30 highly branched isoprenoid alkenes in laboratory cultures of two marine diatoms. *Organic Geochemistry* 21, 407-413.

Wang, J., Cota, G.F., Comiso, J.C., 2005. Phytoplankton in the Beaufort and Chukchi Seas: Distribution, dynamics, and environmental forcing. *Deep Sea Research II* 52, 3355-3368.

Wuchter, C., Schouten, S., Coolen, M.J.L., Sinninghe Damsté, J.S., 2004. Temperature-dependent variation in the distribution of tetraether membrane lipids of marine Crenarchaeota: Implications for TEX_{86} paleothermometry. *Paleoceanography* 19, PA4028.

Wuchter, C., Schouten, S., Wakeham, S.G., Sinninghe Damsté, J.S., 2006. Archaeal tetraether membrane lipid fluxes in the northeastern Pacific and the Arabian Sea: Implications for TEX_{86} paleothermometry. *Paleoceanography* 21, PA4208, doi:10.1029/2006PA001279.

Wraige, E.J., Belt, S.T., Lewis, C.A., Cooke, D.A., Robert, J.-M., Masse, G., Rowland, S.J., 1997. Variations in structure and distributions of C_{25} highly branched isoprenoid (HBI) alkenes in cultures of the diatom, *Haslea ostrearia* (Simonsen). *Organic Geochemistry* 27, 497-505.

Wraige, E.J., Belt, S.T., Masse, G., Robert, J.-M., Rowland, S.J., 1998. Variations in distributions of C_{25} highly branched isoprenoid (HBI) alkenes in the diatom, *Haslea ostrearia*: influence of salinity. *Organic Geochemistry* 28, 855-859.

Xu, Y., Jaffé, R., Wachnicka, A., Gaiser, E.E., 2006. Occurrence of C_{25} highly branched isoprenoids (HBIs) in Florida Bay: Paleoenvironmental indicators of diatom derived organic matter inputs. *Organic Geochemistry* 37, 847-859.